The external pore loop interacts with S6 and S3-S4 linker in domain 4 to assume an essential role in gating control and anticonvulsant action in the Na^+ channel

Ya-Chin Yang,[1] Jui-Yi Hsieh,[2] and Chung-Chin Kuo[2,3]

[1]Department of Life Science, Chang-Gung University, Tao-Yuan 333, Taiwan
[2]Department of Physiology, National Taiwan University College of Medicine, and [3]Department of Neurology, National Taiwan University Hospital, Taipei 100, Taiwan

Carbamazepine, phenytoin, and lamotrigine are widely prescribed anticonvulsants in neurological clinics. These drugs bind to the same receptor site, probably with the diphenyl motif in their structure, to inhibit the Na^+ channel. However, the location of the drug receptor remains controversial. In this study, we demonstrate close proximity and potential interaction between an external aromatic residue (W1716 in the external pore loop) and an internal aromatic residue (F1764 in the pore-lining part of the sixth transmembrane segment, S6) of domain 4 (D4), both being closely related to anticonvulsant and/or local anesthetic binding to the Na^+ channel. Double-mutant cycle analysis reveals significant cooperativity between the two phenyl residues for anticonvulsant binding. Concomitant F1764C mutation evidently decreases the susceptibility of W1716C to external Cd^{2+} and membrane-impermeable methanethiosulfonate reagents. Also, the W1716E/F1764R and G1715E/F1764R double mutations significantly alter the selectivity for Na^+ over K^+ and markedly shift the activation curve, respectively. W1716 and F1764 therefore very likely form a link connecting the outer and inner compartments of the Na^+ channel pore (in addition to the selectivity filter). Anticonvulsants and local anesthetics may well traverse this "S6 recess" without trespassing on the selectivity filter. Furthermore, we found that Y1618K, a point mutation in the S3-4 linker (the extracellular extension of D4S4), significantly alters the consequences of carbamazepine binding to the Na^+ channel. The effect of Y1618K mutation, however, is abolished by concomitant point mutations in the vicinity of Y1618, but not by those in the internally located inactivation machinery, supporting a direct local rather than a long-range allosteric action. Moreover, Y1618 could interact with D4 pore residues W1716 and L1719 to have a profound effect on both channel gating and anticonvulsant action. We conclude that there are direct interactions among the external S3-4 linker, the external pore loop, and the internal S6 segment in D4, making the external pore loop a pivotal point critically coordinating ion permeation, gating, and anticonvulsant binding in the Na^+ channel.

INTRODUCTION

Many widely prescribed anticonvulsants and local anesthetics are use-dependent inhibitors of neuronal Na^+ channels. These drugs bind preferentially, although with slow kinetics, to the inactivated rather than to the resting state of the voltage-gated Na^+ channel (Lipicky et al., 1972; Hille, 1977; Courtney et al., 1978; Bean et al., 1983; Matsuki et al., 1984; Willow et al., 1985; Schwartz and Grigat, 1989; Butterworth and Strichartz, 1990; Lang et al., 1993; Kuo and Bean, 1994; Xie et al., 1995; Kuo et al., 1997; Kuo and Lu, 1997). Na^+ currents and cellular excitability are therefore decreased in a voltage- and time-dependent fashion. A common receptor for these drugs has long been implicated (Kuo, 1998a; Kuo et al., 2000; see also Ragsdale et al., 1996), but the exact location of the drug receptor, as well as the gating conformational changes essential for drug receptor modulation, remains unsettled. Point mutation studies suggested that F1764 ($Na_v1.2$ numbering) near the middle of the sixth transmembrane segment (S6) in domain 4 (D4S6) is crucial for the binding of both local anesthetics and anticonvulsants (Ragsdale et al., 1994, 1996; McNulty et al., 2007). Similar findings have also been documented for the S6s in the other domains (Yarov-Yarovoy et al., 2001, 2002). These findings led to a proposal of an internal location of the drug receptor. Unfortunately, most of the aforementioned mutations also cause gating changes (Ragsdale et al., 1994; Yarov-Yarovoy et al., 2001; unpublished data), raising a concern of allosteric rather than direct modification of the drug receptor by mutations. On the other hand, there are also experimental evidences indicative of an external site for drug binding. For instance, functional

Correspondence to Chung-Chin Kuo: chungchinkuo@ntu.edu.tw

Abbreviations used in this paper: MTSEA, 2-aminoethyl-methanethiosulfonate; MTSES, ethylsulfonate-methanethiosulfonate; MTSET, ethyltrimethylammonium-methanethiosulfonate; RIIA, rat brain type IIA.

The Rockefeller University Press $30.00
J. Gen. Physiol. Vol. 134 No. 2 95–113
www.jgp.org/cgi/doi/10.1085/jgp.200810158

data with intracellular application of phenytoin, carbamazepine, and lamotrigine suggest that the anticonvulsants should bind to the external side of the cell (Kuo, 1998a). Moreover, point mutations of the external residues (e.g., in the external part of D4S6 or in the D4 external pore loop, the latter being equivalent to W1716 in $Na_v1.2$) would significantly alter the access of external QX-314 and local anesthetics binding to the channel pore (Ragsdale et al., 1994; Qu et al., 1995; Wang et al., 1998; Lee et al., 2001; Tsang et al., 2005). Binding assays of [^{3}H]BW202W92 of the lamotrigine family also support an external binding site for the anticonvulsants (Riddall et al., 2006). Most intriguingly, occupancy of the external pore mouth of Na^+ channels by external Na^+ would delicately alter the local geometry to make diclofenac (a structural analogue of carbamazepine and also an inactivation stabilizer of the channel) an opportunistic blocker of the pore (Yang and Kuo, 2005). Consistently, Tikhonov and Zhorov (2007) also proposed that occupation of the DEKA ring by Na^+ would antagonize binding of local anesthetics. These latter findings strongly suggest significant interaction between the external pore loop and the binding site for local anesthetics and anticonvulsants, and thus an external location of the binding site in the Na^+ channel.

We have suggested that there are continuous conformational changes of the anticonvulsant receptor with Na^+ channel activation and inactivation (Yang and Kuo, 2002, 2005). However, how the anticonvulsant receptor is "shaped" with the voltage-dependent gating process remains obscure. Intuitively, the linkers directly connected to S4s could be responsible for transducing membrane voltage to the conformational changes of the channel gates and the drug receptor. If the anticonvulsant receptor is in the internal part of the pore and formed by S6, it is conceivable that the possible inter- and intra-subunit interactions between the S4-S5 linker and the S6 in the K^+ and Na^+ channels may play a role in the modulation of receptor conformation (McPhee et al., 1995, 1998; Tang et al., 1996; Popa et al., 2004; Long et al., 2005a,b). If the receptor is in the external vestibule, it would be interesting to note that S4 would move close to the external pore region in K^+ channels (Li-Smerin and Swartz, 2000; Elinder et al., 2001; Gandhi et al., 2003; Laine et al., 2003). A recent study also proposed that the S3-S4 linker of domain 2 is in close proximity to the pore loop of domain 3 in Nav1.4 channel (Cohen et al., 2007). Moreover, mutations or pore blockers in the external vestibule have been repeatedly reported to affect activation and inactivation in K^+ and Na^+ channels (Tomaselli et al., 1995; Kuo, 1998b; Townsend and Horn, 1999; Hilber et al., 2001; Kuo et al., 2004). In the present study, we propose a solution to the apparently perplexing or even conflicting reports on the location of the drug receptor and provide novel structural insight into the molecular organization of the Na^+ channel. We found that the common drug receptor should involve both W1716 in the external pore loop (SS6) and F1764 in the internal pore compartment of S6 in domain 4. The interaction between these two phenyl residues constitutes a "recess" that makes a second link in addition to the selectivity filter between the inner and outer compartments of the pore. We further demonstrated the close proximity and interaction between D4S3-4 linker and SS6 external pore segment, constituting an imperative element closely related to channel activation, inactivation, and the anticonvulsant drug action. We conclude that the D4SS6 pore loop segment is in a pivotal position coordinating major physiological attributes (activation, inactivation, and ion permeation) as well as pharmacological modulations (the receptor for anticonvulsants and local anesthetics) of the Na^+ channel chiefly via its intimate interactions with the D4S6 segment and the D4S3-4 linker.

MATERIALS AND METHODS

Molecular biology and expression of Na^+ channels

The plasmid pNa200 encoding the rat brain type IIA (RIIA) Na^+ channel was provided by A.L. Goldin (University of California, Irvine, Irvine, CA). The RIIA ($Na_v1.2$) channel is chosen for the correlation of our data with those previously documented in native Na^+ channels in rat central neurons. Side-directed mutagenesis in the RIIA Na^+ channel was performed with the QuikChange mutagenesis system (Agilent Technologies). The mutation-containing pNa200 was linearized with NotI restriction enzyme, and RNA transcripts for oocyte expression were synthesized using the T7 mMESSAGE mMACHINE transcription kit (Applied Biosystems). Mature female *Xenopus laevis* frogs were maintained and handled under the supervision of National Taiwan University College of Medicine and College of Public Health Institutional Animal Care and Use Committee. For oocyte isolation, the animals were anaesthetized and the ovarian sacs were removed. The frogs were allowed to recover in a water tank at room temperature immediately after the surgery. Isolated and defolliculated oocytes (stages V–VI) were injected with cRNA transcripts and maintained at 18°C for 1–7 d before electrophysiological studies.

Two-electrode intracellular recording

Macroscopic Na^+ currents in oocytes were recorded by a standard two-microelectrode voltage clamp method. The oocyte was put in a chamber continuously perfused with modified ND-96 solution (in mM: 96 NaCl, 4 KCl, 1 $MgCl_2$, 0.3 $CaCl_2$, and 5 HEPES, pH 7.6). 2-aminoethyl-methanethiosulfonate (MTSEA), ethylsulfonate-methanethiosulfonate (MTSES), and ethyltrimethylammonium-methanethiosulfonate (MTSET; Toronto Research Chemicals) were stocked at −70°C and dissolved in water to make 100 mM of aqueous stock solution that was freshly prepared daily, stored at −20°C, and diluted immediately before use. Both voltage-sensing and current-passing electrodes were filled with 3 M KCl and had a serial resistance of 0.1–0.4 MΩ. Membrane potential was controlled by a two-electrode voltage clamp amplifier with a virtual ground circuit (model OC-725C; Warner Instrument). Data were recorded at room temperature of ~25°C and digitized at 20–100-µs intervals using a Digidata-1200 analogue/digital interface and pCLAMP software (MDS Analytical Technologies). All statistics are given as mean ± SE of mean. To plot the inactivation curves, the oocyte was held at −120 mV and stepped to the inactivating

pulse (for the pulse duration, see figure legends). The peak current elicited by a test pulse to 0 mV for 10 ms after each inactivating pulse is normalized to the peak current with an inactivating pulse at −120 mV and plotted against the voltage of the inactivating pulse (V) to obtain the inactivation curves. The data are fitted with a Boltzmann function $1/(1 + \exp((V-V_{1/2})/k))$, where $V_{1/2}$ is the half-inactivating potential and k is the slope factor. To plot the activation curves (i.e., the normalized conductance–voltage curves), the oocyte was stepped to different test voltages from a holding potential of −120 mV to obtain the current–voltage plot. The maximal conductance is determined by a regression line of the data points between the largest inward current and the zero-current point of the current–voltage plot. The current–voltage plot is normalized to this regression line to give the normalized conductance–voltage curve, which is fitted with a Boltzmann function $1/(1 + \exp((V_{1/2}-V)/k))$. $V_{1/2}$ is the half-activating potential and k is the slope factor.

RESULTS

Point mutations of W1716 and F1764 decrease the affinity of carbamazepine to the inactivated Na^+ channel in a non-additive manner

We have demonstrated that anticonvulsants phenytoin, carbamazepine, and lamotrigine bind to a common receptor with their shared diphenyl structural motif (Kuo, 1998a; Kuo et al., 2000). In this regard, it is intriguing that an external aromatic residue W1716 and an internal aromatic residue F1764 ($Na_v1.2$ numbering) were both reported to affect the apparent binding affinities of anticonvulsants and/or local anesthetics (Ragsdale et al., 1994, 1996; Tsang et al., 2005; McNulty et al., 2007). We thus examined possible interactions between the two residues. The binding affinity of carbamazepine to the inactivated channel (relative to that to the resting channel) was characterized by a shift of the inactivation curve (Bean et al., 1983; Bean, 1984). Mutation of W1716 or F1764 into either alanine or cysteine evidently decreases the affinity of carbamazepine to the inactivated Na^+ channel (Table I). Double-mutant cycle analyses (Carter et al., 1984) reveal that all of the double mutations tested (W1716A/F1764A, W1716A/F1764C, W1716C/F1764A, and W1716C/F1764C) cannot have additive effects in terms of drug affinity changes, suggesting a significant interaction between the two residues contributing to drug binding. It is interesting that the calculated pairwise interaction energies ($\Delta\Delta G_{inter}$) between a W1716 mutant and a F1764 mutant are always close to ∼0.35 kcal/mol (Table I), reminiscent of a recent finding of the interaction energies between aromatic side chains in OmpA channel (a gated channel from *Escherichia coli*; Hong et al., 2007).

The inactivation-stabilizing effect and the external Cd^{2+} sensitivity of W1716C are abolished by mutation F1764C

In addition to the non-additive effect on drug affinity change, there are also interesting alterations in the gating curves of the forgoing double-mutant channels. The gating curves of W1716C, F1764C, and W1716C plus F1764C (W1716C/F1764C) mutant channels are compared in Fig. 1 A. The activation and inactivation curves in F1764C mutant channels are similar to the wild-type curves (with a difference in $V_{1/2}$ of no more than 5 mV in both cases), implying that channel gating remains largely unaffected with the mutation. On the other hand, W1716C mutation evidently shifts the inactivation curve by ∼10 mV without significantly altering the activation curve (Fig. 1 A). Interestingly, the left shift of the inactivation curve by W1716C is "corrected" by the concomitant mutation F1764C (Fig. 1 A, right), again implying a significant interaction between the two residues. Despite the restored inactivation properties, the W1716C/F1764C double mutation still significantly affects the action of the inactivation stabilizer carbamazepine (Table I). The drug

TABLE I

Decrease of the relative binding affinity of carbamazepine to the inactivated Na^+ channel by W1716 and/or F1764 mutations

	Decrease in $V_{1/2}$ shift (mV)	ΔΔG (meV)	ΔΔG (Kcal)	$\Delta\Delta G_{inter}$ (Kcal)
F1764A	4.8 ± 0.36	20	0.46	
F1764C	4.3 ± 0.76	17.9	0.41	
W1716A	0.75 ± 0.29	3.2	0.074	
W1716C	4.0 ± 0.72	16.7	0.38	
F1764A + W1716A	1.8 ± 0.15	7.5	0.17	−0.36
F1764A + W1716C	5.0 ± 0.049	20.9	0.48	−0.36
F1764C + W1716A	1.2 ± 0.19	5	0.12	−0.36
F1764C + W1716C	4.7 ± 0.065	19.6	0.45	−0.34

The inactivation curves were done by the protocols described in Materials and methods and are fitted with a Boltzmann function $1/(1 + \exp((V-V_{1/2})/k))$. For the sake of simplicity, we fixed the slope factor k to determine the shift of $V_{1/2}$ (the difference between $V_{1/2}$ values in the presence and absence of 100 μM carbamazepine). This simplification seems to be appropriate, as the slope of the curve does not greatly differ among these mutations either in the presence or absence of carbamazepine. $V_{1/2}$ shift of the wild-type channel is 6.1 ± 0.2 mV. The decrease in $V_{1/2}$ shift by mutation is then given as the difference between the shift in each mutant and 6.1 mV. The free energy change (ΔΔG) is directly derived from the product of the decrease in $V_{1/2}$ shift and the apparent equivalent gating charges (derived from RT/Fk or 25 mV/k). The interaction energy $\Delta\Delta G_{inter}$ is equal to the ΔΔG in the double mutant minus the summation of ΔΔG in each component single mutant. All of the $\Delta\Delta G_{inter}$ values are significantly smaller than zero, strongly suggesting the non-additive nature for W1716 and F1764 mutations to alter the drug binding affinity.

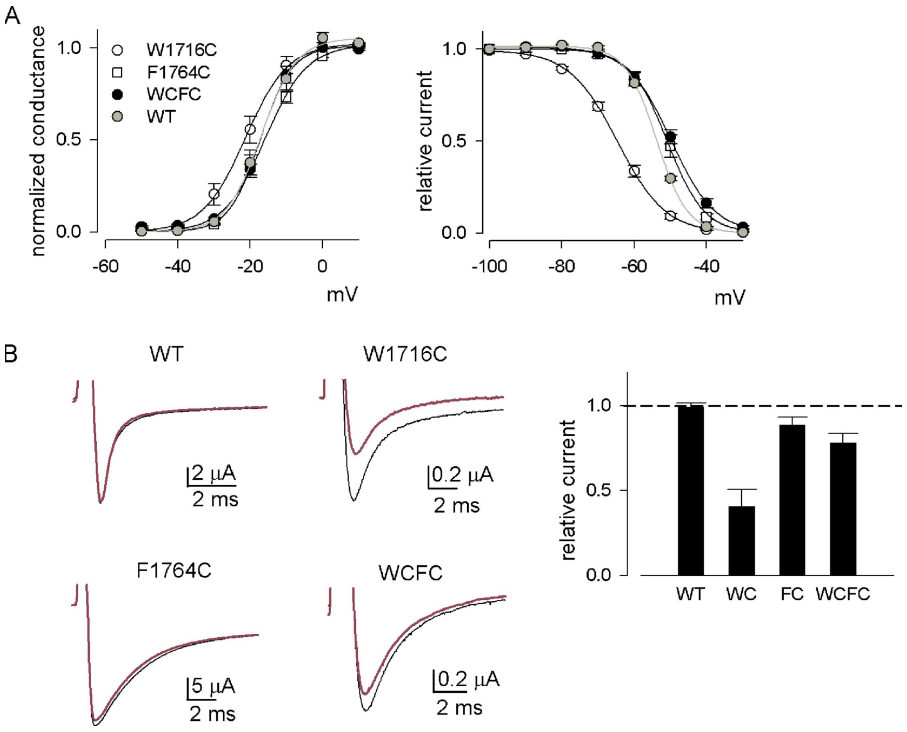

Figure 1. The gating curves and Cd^{2+} block in the W1716C/F1764C (WCFC) double-mutant and the corresponding single-mutant channels. (A) The activation curves (left) and the inactivation curves (right) were documented by the protocols described in Materials and methods. The duration of the inactivating pulse for plotting the inactivation curve is set at 5 s to facilitate comparison with the data (Table I) in the presence of drugs that have relatively slow binding kinetics. The findings remain qualitatively very similar with 100-ms inactivating pulses (not depicted). The curves in the left panel are fits with a Boltzmann function with $V_{1/2}$ values (in mV) of −16.9, −21.3, −15.9, and −17.2 and k values of 4.9, 5.9, 5.7, and 4.4 for the wild-type (WT; the gray line, n = 6), W1716C (n = 6), F1764C (n = 17), and WCFC (n = 15) mutant channels, respectively. The curves in the right panel are fits with a Boltzmann function with $V_{1/2}$ values (in mV) of −54.2, −64.6, −50.9, and −49.8 and k values of 4.6, 6.7, 5.1, and 6.1 for the WT (the gray line, n = 10), W1716C (n = 7), F1764C (n = 4), and WCFC (n = 14) mutant channels, respectively. (B) Cd^{2+} block of different mutant channels. The oocyte was held at −110 mV and stepped every 3 s to a test pulse of −20 mV for 100 ms. (Left) The elicited currents in the presence (red lines) and absence (black lines) of 100 µM Cd^{2+}. (Right) The peak currents in the former are normalized to the peak current in the latter to give the relative current (n = 4–7).

affinity changes characterized in Table I thus are unlikely ascribable to altered channel inactivation. Because both local anesthetics and anticonvulsants are pore blockers of the Na^+ channel, the key ligands responsible for drug binding should be capable of facing the pore. In this regard, W1716C, an additional cysteine in the external pore loop, indeed greatly increases the affinity of external pore blocker Cd^{2+} to the channel (Fig. 1 B). Interestingly, the increase of Cd^{2+} affinity with W1716C mutation is again largely abolished by the addition of a second cysteine substitution for F1764. It is apparently counterintuitive that one more cysteine in the pore would lead to less Cd^{2+} block of the channel. This finding is, however, consistent with a direct or allosteric interaction between the two added cysteines (W1716C and F1764C), altering the local geometry of W1716C and consequently its sensitivity to external Cd^{2+}.

F1764C abolishes the accessibility of W1716C to different external MTS derivatives

We further tested the sensitivity of W1716C to different hydrophilic MTS reagents and examined whether it can also be influenced by manipulation of F1764 (Fig. 2). Fig. 2 A shows that the W1716C channel, but not the F1764C channel, can be modified by externally applied MTSET, a positively charged sulfhydryl reagent, at moderately depolarized membrane potentials such as −35 mV. These findings are consistent with the report that point mutations I1575C, F1579C, and V1583C in the skeletal muscle Na^+ channel (equivalent to I1760, F1764, and V1768 in Nav1.2 and presumably facing the same side in the S6 α-helix) could not be effectively modified by saturating concentrations (∼2 mM) of MTSET (Vedantham and Cannon, 2000; Sunami et al., 2001, 2004). W1716C thus should indeed face the external part of the pore, whereas F1764C is not accessible to MTSET from the outside. In this regard, it is interesting that the rate, and even more dramatically the steady-state extent, of MTSET modification of W1716C is decreased by the concomitant mutation F1764C (Fig. 2, B and C). Also, the state-dependent modification by MTSET is less obvious in the W1716C/F1764C double-mutant channel compared with the single W1716C mutant channel (i.e., the inhibition is equally small in the double-mutant channel at −35 and −110 mV, but is much stronger at −35 than at −110 mV in the W1716C single-mutant channel; unpublished data). These findings strongly support an altered local conformation or reactivity of the cysteine side chain at position 1716 in the concomitant presence of the other cysteine at position 1764. In contrast to the case of MTSET, we found that F1764C is modifiable by external MTSEA, a usually uncharged agent with a smaller size than that of MTSET (not depicted). However, MTSEA decreases only the late sustained phase (not the peak) of the current, suggesting an altered channel inactivation rather than a blocking of the passage of

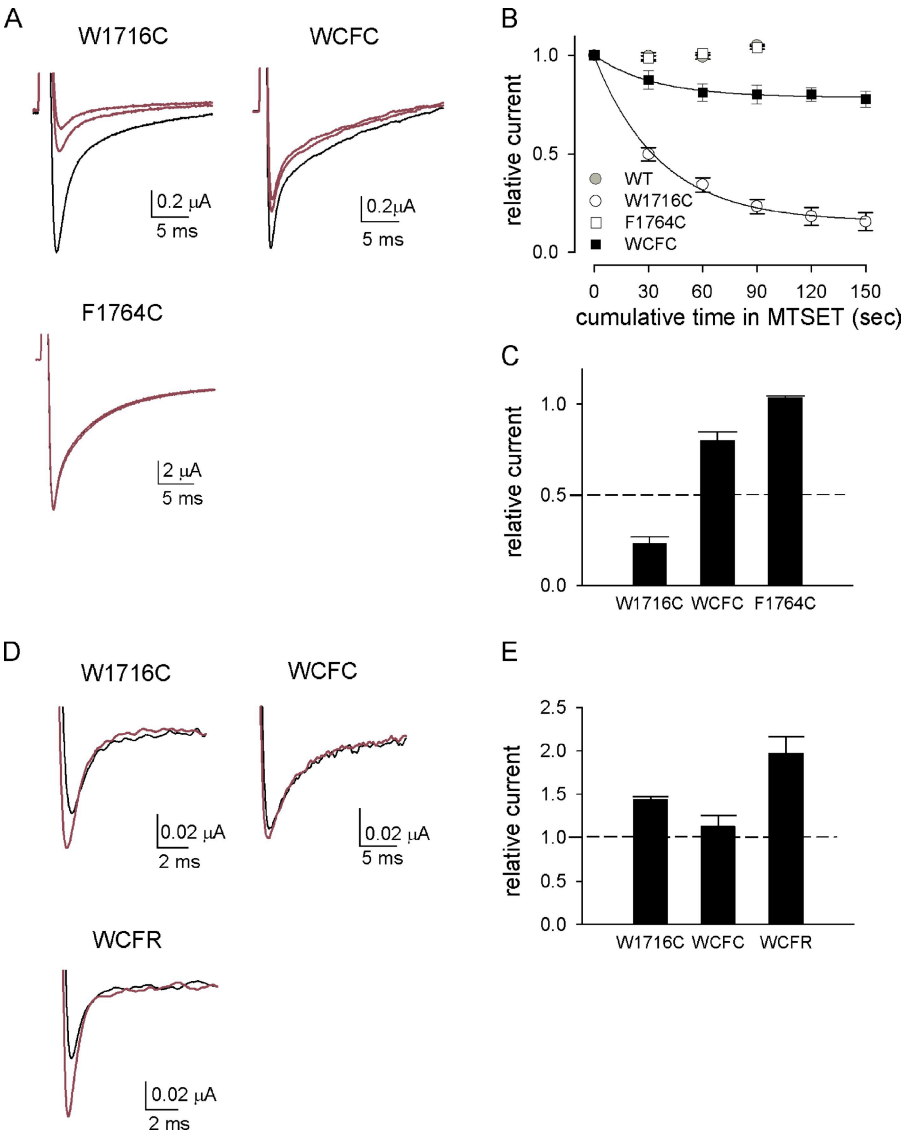

Figure 2. The effect of external MTSET and MTSES on the wild-type, W1716C, F1764C, and W1716C/F1764C (WCFC) or W1716C/F1764R (WCFR) mutant channels. (A) The effect of external MTSET. (Left) The sample currents after 0- (black line), 60-, and 120-s (red lines) cumulative modification by MTSET are shown. The oocyte was initially held at −110 mV and stepped to −10 mV for 40 ms to elicit the control Na^+ currents in ND-96 solution. The oocyte was then held at −35 mV and perfused with ND-96 containing 0.1 mM (for W1716C and WCFC mutant channels) or 1 mM (for wild-type and F1764C mutant channels) of freshly made MTSET for 30 s, after which the oocyte was held at −110 mV again and washed with control ND-96 for 30–60 s. The Na^+ current after modification was assessed by a test pulse at −10 mV. This protocol was repeated until a steady state of MTSET modification was reached. We also repeated the same experimental protocols in the absence of MTS reagents and found no changes in the currents before and after the protocols (not depicted). (B) The relative currents are plotted against the cumulative time in MTSET (n = 3–4). The curves are relative current = 0.84 × exp(−t/36.2) + 0.16 and relative current = 0.22 × exp(−t/32.8) + 0.78 for the W1716C and WCFC mutant channels, respectively, where t denotes the cumulative time in MTSET in seconds. (C) Peak Na^+ currents after 90-s MTSET modification is normalized to control currents to give the relative currents (n = 3–4). (D) The effect of external MTSES. The oocyte was held at −120 mV, perfused with control ND-96 solution or ND-96 solution containing 2 mM of freshly made MTSES, and stepped every 2 s to −10 mV for 100 ms to assess the Na^+ currents. A steady-state effect of MTSES is usually reached within 40 s in these mutant channels (not depicted). The oocyte was then washed with control ND-96 for 30–60 s and stepped to −10 mV to measure the Na^+ current. The Na^+ currents after 0- (black line) and 40-s (red line) cumulative modification by MTSES are superimposed. (E) Peak Na^+ currents after a 40-s MTSES modification are normalized to control currents to give the relative currents (n = 3–4).

permeating ions. We also examined whether the accessibility of W1716C to the presumably negatively charged agent MTSES is altered by F1764C (Fig. 2, D and E). MTSES-modified W1716C channels represent an increase rather than decrease in current amplitude (examined at −10 mV). Nevertheless, F1764C still decreases the accessibility of W1716C to MTSES, and the current amplitude is restored (in the W1716C/F1764C double-mutant channel; Fig. 2, D and E). Thus, F1764C abolishes the accessibility of W1716C to different external agents (Cd^{2+}, MTSET, and MTSES) regardless of their different chemical properties and different mechanisms of actions. Other than the cysteine–cysteine cross-linking, the close proximity of W1716 and F1716 is also supported by the significant electrostatic interaction if countercharges are introduced to these two positions. For example, the current amplitude is also increased by MTSES modification in the W1716C/F1764R mutant channel, and the increase is even larger than that in the W1716C single mutant (Fig. 2, D and E). It seems that both the shorter cysteine–cysteine cross-linking and the much longer-range linkage via MTSES-arginine (electrostatic) interactions between W1716 and F1716 are capable of twisting the position of W1716 and/or the adjacent pore loop to a different geometry (see below).

The selectivity for Na^+ is altered by W1716E/F1764R double mutation

We next tested whether a salt bridge can be formed between F1764R and W1716E, the side-chain length of

which is shorter than that of the MTSES adduct attached to W1716C. If W1716 faces the pore, mutations at this position may affect ion passage or even ion selectivity of the channel (see also Tsushima et al., 1997). We found that W1716C and W1716A mutations indeed shift the reversal potential by ~20–30 mV (characterized by conventional two-electrode intracellular recording with ND-96 external solution; unpublished data), whereas the W1716E mutant channel has a reversal potential similar to the wild-type channel (different by only ~5 mV; Fig. 3 A). We did not observe currents from the W1716R mutant channel. On the other hand, mutations of F1764 (e.g., F1764A, F1764C, and F1764E) tend to cause only relatively small change in the reversal potential (changes of ~1–12 mV; unpublished data). Notably, the F1764R mutant channel has a reversal potential very similar to that of the wild-type channel (Fig. 3, A and B). Although either W1716E or F1764R single mutation negligibly affects the reversal potential, the W1716E/F1764R double-mutant channel has a very dramatic shift (~40 mV) in the reversal potential, nearly abolishing the selectivity for Na^+ over K^+ (i.e., the reversal potential is close to 0 mV; Fig. 3 A with the oocyte bathed in ND-96 solution). These findings are consistent with the idea that that W1716 faces the pore and is closely associated with the selectivity filter. Moreover, there is very likely a direct and significant interaction (e.g., a salt bridge) between W1716E and F1764R, critically altering the conformation of the pore loop and consequently ion selectivity.

The activation curve shows a large rightward shift with countercharges introduced at G1715 and F1764

The selectivity change in the W1716E/F1764R double-mutant channel in Fig. 3 suggests close proximity between the SS6 pore-lining segment and the internal segment of the S6 helix. If so, and if the pore loop has a more flexible secondary structure than α-helix or β-sheet, a similar interaction might be obtained in the adjacent residues. We thus introduced a glutamate to G1715, a residue next to W1716 and just external to A1714 of the presumable selectivity filter (i.e., the DEKA ring). We found that neither the G1715E single-mutant channel nor the G1715E/F1764R double-mutant channel significantly changes the ion selectivity (not depicted). However, the G1715E/F1764R double mutation leads to a dramatic rightward shift in the activation curve, whereas the F1764R single mutation does not shift the curve significantly, and the G1715E single mutation even causes a slight leftward shift (Fig. 4, left). In contrast, the inactivation curves of these mutant channels are essentially unchanged (with either 100-ms or 5-s inactivating pulses; Fig. 4, right, and unpublished data). These findings suggest a significant interaction between G1715E and F1764R, causing a much more stabilized resting (deactivated) than activated conformation and probably even dissociation of inactivation from activation, and provide further support for the close proximity between the pore loop and S6 in domain 4. Interestingly, we found that the L1719E plus F1764R double mutation also causes a rightward shift (~10-mV shift) of the activation curve, but not the inactivation curve (not depicted). It is also intriguing that a structural twist of S6 constrained by the P loop in domain 4 would affect activation rather than inactivation, considering that D4S6 is primarily seen as an inactivation apparatus (e.g., W1716C shifts the inactivation rather than the activation curves; Fig. 1 A). This may imply the

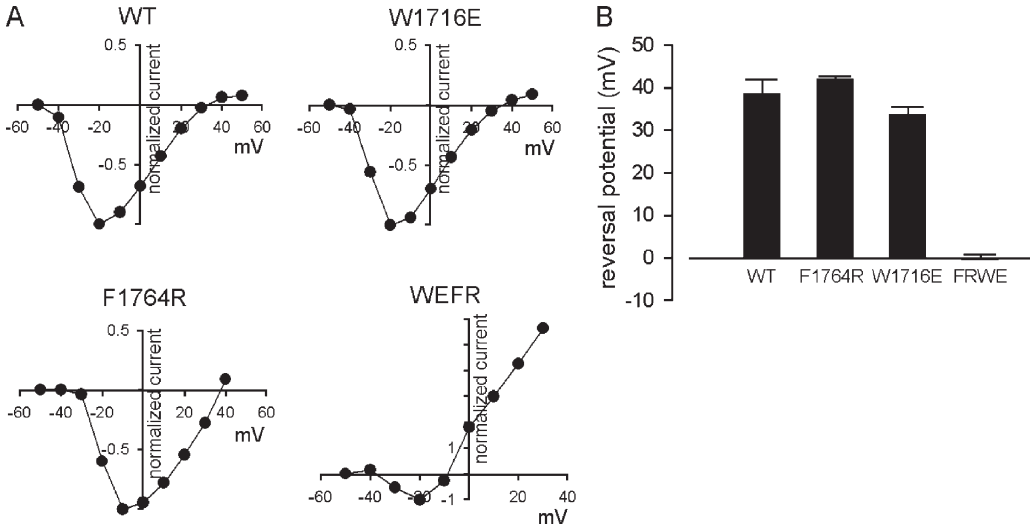

Figure 3. The reversal potentials in the wild-type (WT), W1716E, F1764R, and W1716E/F1764R (WEFR) mutant channels. (A) The representative current–voltage plots. The oocytes expressing each of the four different channels were bathed in ND-96. The oocytes were held at −120 mV and stepped to a test pulse of −120 to +50 mV for 100 ms, and then returned to −120 mV. The pulse protocols were repeated every 3 s, and the peak current at each test pulse is normalized to the maximal current elicited and plotted against the test pulse voltage to give the current–voltage plots. (B) The averaged reversal potentials for the four different channels in A (n = 5–15).

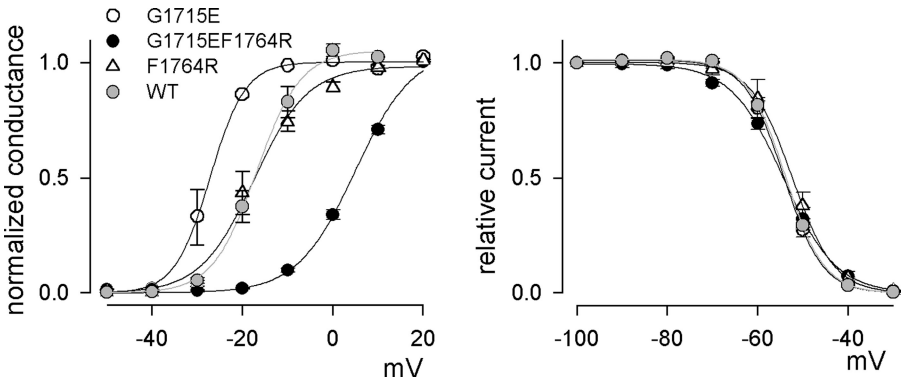

Figure 4. The gating curves in the wild-type (WT), G1715E, F1764R, and G1715E/F1764R (GEFR) mutant channels. The activation (left) and inactivation curves (right; inactivating pulse duration = 5 s) were documented by the protocols described in Materials and methods. The data for the wild-type channel are from Fig. 1 A and shown as gray symbols with gray lines. The activation curves are fits with a Boltzmann function with $V_{1/2}$ values (in mV) of −27.2, −17.5, and 4.9 and k values of 3.9, 5.9, and 6.4 for G1715E ($n = 3$), F1764R ($n = 6$), and GEFR ($n = 7$) mutant channels, respectively. The inactivation curves are fits with a Boltzmann function with $V_{1/2}$ values (in mV) of −54.2, −52.3, and −54.2 and k values of 4.3, 4.6, and 5.8 for G1715E ($n = 6$), F1764R ($n = 8$), and GEFR ($n = 6$) mutant channels, respectively.

involvement of the external pore loop of domain 4 in the coupling of channel activation and inactivation (see below). These findings indicate that the structural arrangement in the vicinity of SS6 and the adjacent S6 is critical for the proper functional attributes of the Na^+ channel, including activation, inactivation, and ion permeation.

Carbamazepine retards macroscopic inactivation of the Na^+ channel with mutations of an aromatic residue Y1618 in the S3-4 linker of domain 4

We have demonstrated that the interaction between D4SS6 and D4S6 in the Na^+ channel is crucial for drug receptor formation and appropriate channel gating, both being attributes closely associated with the membrane voltage. Because there is a tight correlation between D4S4 and channel inactivation (Stühmer et al., 1989; Chahine et al., 1994; Chen et al., 1996; Kühn and Greeff, 1999; Sheets et al., 1999; Yang and Kuo, 2003), and the interaction between the "inactivation-stabilizing" anticonvulsants and their receptor site most likely involves the diphenyl structural motif (Kuo, 1998a; Kuo et al., 2000), we searched the aromatic amino acid residues in the regions that are likely to be affected by the movement of the D4S4 voltage sensor. We found that lysine substitution for a tyrosine residue (Y1618) in the D4S3-S4 linker, a short extracellular extension of D4S4, would intriguingly alter the action of carbamazepine. As carbamazepine is also a pore blocker of the wild-type Na^+ channel, the macroscopic current decay is significantly accelerated with a high concentration of the drug (Yang and Kuo, 2002). However, carbamazepine retards the fast decay phase of the macroscopic Na^+ current in the Y1618K mutant channel (Fig. 5 A). This apparently simple finding has two important implications. First, carbamazepine is no longer an effective pore blocker of the Na^+ channel. Otherwise, binding of the drug would immediately result in current reduction, incompatible with the actual current "augmentation" during essentially the whole phase of current decay (Fig. 5 A). Second, at least in the Y1618K mutant channel, the binding of carbamazepine slows the kinetics of inactivation but still "stabilizes" the inactivated state over the resting state of the channel (see also Fig. 6). In other words, change of a presumably externally located aromatic residue in the D4S3-4 linker could significantly alter the conformation of the anticonvulsant binding site in the pore, and drug binding to the altered receptor now has a deterring effect on the operation of the inactivation machinery. We found that carbamazepine also has a slowing effect on macroscopic current decay in the other mutant channels with charge-containing substitutions for Y1618, such as Y1618D and Y1618R (albeit to a lesser extent than Y1618K; Fig. 5 B). On the other hand, carbamazepine accelerates the macroscopic current decay when Y1618 is mutated to tryptophan (Y1618W, a plainer aromatic residue), but not to proline and alanine (Y1618P and Y1618A; Fig. 5 B; the absolute values of the decay rates for the wild-type and different Y1618 mutant channels without drugs are given in Table II). These findings argue for a close and delicate association of Y1618 with the conformation of the anticonvulsant binding site, and thus small differences among the substituted side chains at this position would so differently alter the local binding geometry of the anticonvulsant and consequently the action of carbamazepine on the channel.

Y1618K mutation probably increases the affinity of carbamazepine to the resting Na^+ channel

In view of the significant retardation of macroscopic inactivation (Fig. 5 A), the binding of carbamazepine to the Y1618K mutant channel should happen before channel inactivation. Because of the very low affinity of carbamazepine to the resting wild-type Na^+ channel (Willow et al., 1985; Schwartz and Grigat, 1989; Kuo et al., 1997),

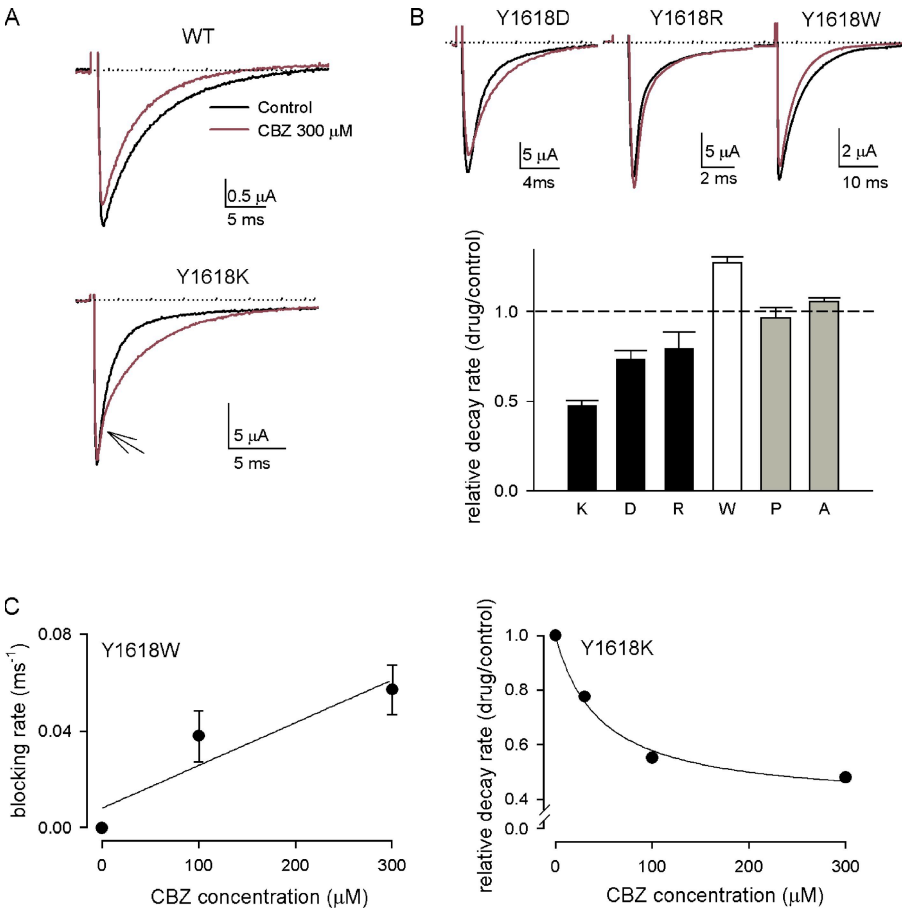

Figure 5. Carbamazepine action on the decay phase of macroscopic Na^+ currents in different Y1618 mutant channels. (A) 300 μM carbamazepine (CBZ) slightly accelerates the decay of the macroscopic current in the wild-type (WT) channel but evidently slows current decay in the Y1618K mutant channel. The two superimposed traces show the representative currents elicited by a step depolarization to +10 mV from a holding potential of −120 mV in the absence (black line) and presence (red line) of 300 μM carbamazepine. The dotted line indicates zero current level. Note that in the Y1618K channel, the slowing of current decay is not discernible from the peak but only becomes evident later on (the arrow indicates an arbitrary "starting point" for the slowing of decay). (B; Top) The same experiments as those in A were repeated in different Y1618 mutant channels. 300 μM carbamazepine (red lines) slightly slows the macroscopic current decay in the Y1618D and Y1618R, yet accelerates the decay in the Y1618W channels. The dotted line indicates zero current level. (Bottom) The relative decay rate (the decay rate in 300 μM carbamazepine normalized to the decay rate in control) is compared among different Y1618 mutant (Y1618K, D, R, W, P, and A) channels (n = 3–9). The decay rate is obtained from the inverse of the time constant of the monoexponential fit to the current decay. (C) Estimation of carbamazepine binding rate to the open Y1618W mutant channels and binding affinity to the resting Y1618K mutant channels. (Left) The differences between the inverses of the current decay time constants in drug and in control are plotted against the concentration of carbamazepine in the Y1618W mutant channel (n = 3). The line is the linear regression fit to the data points of the form: blocking rate (s^{-1}) = 0.177 × D + 8, where D is the concentration of carbamazepine in μM. The slope of the line ($\sim 1.8 \times 10^5\ M^{-1}s^{-1}$) gives a rough estimate of the binding rate of carbamazepine to the open Y1618W channel. (Right) The relative decay rates of the Y1618K mutant channel are plotted against different concentrations of carbamazepine. The relative decay rates in 30, 100, and 300 μM carbamazepine are 0.78 ± 0.028, 0.55 ± 0.046, and 0.48 ± 0.023, respectively (n = 4–9). The error bars are omitted in the plot. The curve is the fit of the data points with a one-to-one binding function: relative decay rate = (1 + 0.38 × D/46.4)/(1 + D/46.4), where D is the concentration of carbamazepine in μM.

one would at first surmise that carbamazepine binds to the activated (open) Y1618K channel to slow subsequent inactivation. Indeed, we have previously reported that carbamazepine binds to the open wild-type Na^+ channel faster than to the inactivated channel (1.10^6 vs. $4 \times 10^4\ M^{-1}s^{-1}$; Yang and Kuo, 2002). In this regard, because carbamazepine evidently accelerates the macroscopic current decay in the Y1618W channel (Fig. 5 B), we roughly estimated the open-channel pore-blocking rate of carbamazepine as $\sim 1.8 \times 10^5\ M^{-1}s^{-1}$ (with an assumption of one-to-one binding of drug to the open channel; Fig. 5 C, left). However, the slowing of macroscopic inactivation by carbamazepine is discernible slightly later than the current peak in the Y1618K channel (i.e., ∼1–2 ms after the start of the depolarizing pulse; see Fig. 5 A). If a binding rate to the open channel is $\sim 1.8 \times 10^5$ to $1.10^6\ M^{-1}s^{-1}$, then 30–300 μM carbamazepine should occupy only a very small fraction of open channels within 1–2 ms. It is thus hard to envisage the manifestation and saturation of the slowing of current decay at 30 μM and 100–300 μM carbamazepine, respectively (Fig. 5 C, right). We therefore propose that carbamazepine more likely binds to the resting Y1618K channel to slow inactivation (also see below for additional evidence). If so, then the concentration-dependent slowing of the decay rate in Fig. 5 C would signal that carbamazepine binds to the resting Y1618K channel with a dissociation constant (K_R) of ∼46 μM, a much higher affinity than that to the resting wild-type channel (>2,000 μM; Kuo et al., 1997). In this case, carbamazepine bound to the resting Y1618K channel might slow down the development of inactivation to ∼38% of that in the drug-free channel (Fig. 5 C, right).

TABLE II

The decay rate of the macroscopic current through the wild-type and different Y1618K mutant channels

	Wild-type	Y1618 single mutants					
		Y1618K	Y1618D	Y1618R	Y1618W	Y1618A	Y1618P
Decay rate (ms^{-1})	0.25 ± 0.05	0.42 ± 0.02	0.78 ± 0.10	0.60 ± 0.10	0.23 ± 0.07	0.56 ± 0.01	0.28 ± 0.03
	Y1618 double mutants						
	Y1618K + F1619K	Y1618K + K1617A	Y1618K + E1616K	Y1618K + R1626C	Y1618K + F1651A		
Decay rate (ms^{-1})	0.45 ± 0.01	0.36 ± 0.01	0.22 ± 0.02	0.21 ± 0.02	0.40 ± 0.03		

The macroscopic current is elicited by a step depolarization to +10 mV from a holding potential of −120 mV. The decay phase of the elicited current is fitted with a monoexponential function, and the inverse of the current decay time constant is given in the table (n = 3–19).

Charged substitutions for Y1618 produces a smaller shift of the inactivation curve by carbamazepine and the other anticonvulsants

It is well established that carbamazepine and the other anticonvulsants preferentially bind to the inactivated rather than the resting wild-type Na^+ channel. If carbamazepine significantly binds to the resting Y1618K channel, it would be desirable to examine the relative binding affinity of the anticonvulsants to the resting versus inactivated Y1618 channels. Fig. 6 A shows an evidently smaller shift of the inactivation curve by 300 μM carbamazepine in the Y1618K, Y1618D, or Y1618R mutant channel than that in the wild-type channel, as if the relative binding affinity of drug to the inactivated over the resting channel is significantly decreased by the charged mutations at Y1618. On the other hand, with the Y1618W mutation, carbamazepine has a similar effect on the inactivation curve to the wild-type case. The extent of inactivation curve shift could be described by:

$$\exp(\Delta V / k) = (1 + D / K_I) / (1 + D / K_R), \quad (1)$$

where ΔV denotes the shift in mV, k is a slope factor obtained from the fit of the curve with a Boltzmann function, and D is the drug concentration (Bean et al., 1983; Bean, 1984). According to Eq. 1 and with a K_R of ∼46 μM (Fig. 4 C), the K_I (the dissociation constant of drug to the inactivated channel) value would be ∼18 μM in the Y1618K mutant, slightly smaller than that in the wild-type channel (∼25 μM; Kuo et al., 1997). These data indicate that charged mutations at Y1618 markedly decrease the differences between the binding affinity of carbamazepine to the inactivated and to the resting channels, consistent with the proposal of altered receptor conformation and increased drug affinity in the resting channel. In this regard, different anticonvulsants presumably bind to a common receptor in the inactivated Na^+ channel with the common diphenyl motif in their structure (Kuo, 1998a; Kuo et al., 2000). If mutations of Y1618 do alter the local geometry of the drug receptor for drug binding, the shift of the inactivation curve by the other anticonvulsants may also be altered by the Y1618 mutation. Similar to carbamazepine, phenytoin and lamotrigine also produce a much smaller shift of the inactivation curve shift in the Y1618K mutant channel than in the wild-type channel (Fig. 6 B). The altered gating conformational changes in the drug receptor with the D4S3-4 linker mutations, together with the different configurations of drug binding in the ion permeation pathways (Fig. 5), would strongly implicate a close relationship among the D4S3-S4 linker, the pore region, and the gating machinery of the Na^+ channel.

The macroscopic inactivation of the Y1618K mutant channel is slowed to different extents by different anticonvulsant drugs

Although the altered shifts in the inactivation curve are very similar among all three anticonvulsants, different anticonvulsants have different slowing effects on the macroscopic inactivation of the Y1618K channel (Fig. 7 A). At a concentration of 100 μM, for example, carbamazepine is the most effective to slow current decay. Phenytoin has a smaller effect, whereas lamotrigine (up to 1 mM) has only a negligible effect in this regard. On the other hand, diclofenac, an antiinflammatory drug that also contains the common diphenyl structure and presumably binds to the same receptor of the anticonvulsants (Yang and Kuo, 2005), also has an inactivation-slowing action roughly comparable to phenytoin. Even in the highest concentration up to the solubility limits, diclofenac, phenytoin, and lamotrigine cannot produce the same extent of inactivation slowing as 100 μM carbamazepine does. Carbamazepine, which contains the most constrained diphenyl motif in a dibenzazepine structure (Kuo et al., 2000), probably most effectively "abducts" the binding ligands in the anticonvulsant receptor to a specific configuration to interfere (kinetically) with the inactivation machinery, whereas lamotrigine, which contains a shortest center-to-center distance between the two phenyl groups (Kuo et al., 2000), is the least capable of doing so. These findings again argue for a very local and direct effect of Y1618 mutations on channel gating.

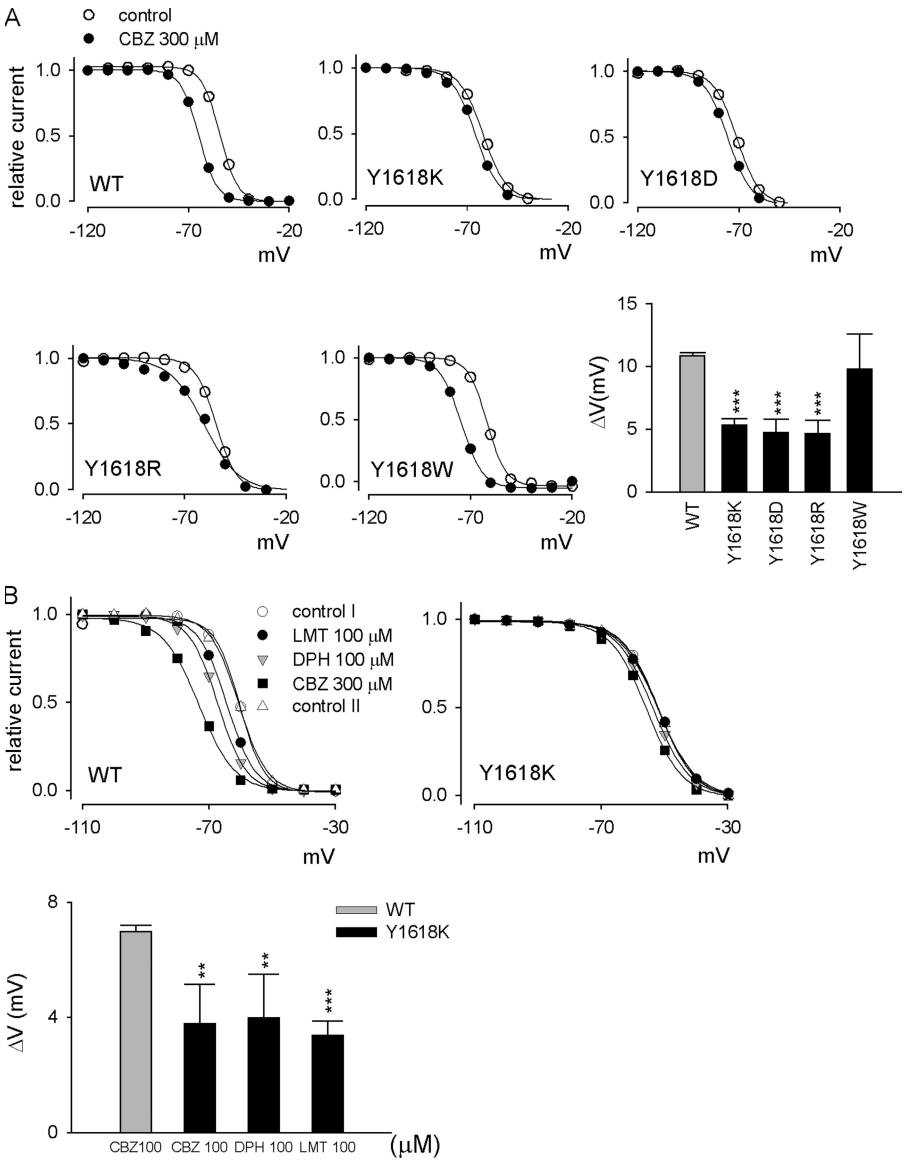

Figure 6. Comparison of the shift of the inactivation curve by carbamazepine and the other anticonvulsant drugs in the wild-type and different Y1618 mutant channels. The inactivating pulse duration was 9 s to make sure of steady-state binding of the anticonvulsants, which have relatively slow binding rates onto the channel. (A) Representative inactivation curves in different Y1618 mutant channels before (open circles) and after (closed circles) the application of 300 μM carbamazepine. The lines are fits with a Boltzmann function with $V_{1/2}$ values (control vs. 300 μM carbamazepine) in mV of −54.4 versus −64.9, −62.2 versus −66.1, −71.5 versus −75.5, −54.7 versus −60.6, and −62.0 versus −74.6, and k values (control vs. carbamazepine) of 4.3 versus 4.5, 5.7 versus 5.7, 5.4 versus 5.7, 5.0 versus 8.3, and 4.5 versus 5.2 for the wild-type (WT), Y1618K, Y1618D, Y1618R, and Y1618W mutant channels, respectively. The shift (ΔV) of the inactivation curve is defined as the difference between the $V_{1/2}$ values in 300 μM carbamazepine and the $V_{1/2}$ value in control and is shown in the bar graph. Mutations Y1618K, Y1618D, and Y1618R, but not Y1618W, evidently decrease the shift of the inactivation curve by carbamazepine ($n = 3$–4). ***, $P < 0.005$ by Student's t test (compared with the wild-type data). (B) The shift of the inactivation curve by phenytoin and lamotrigine in the Y1618K mutant channel. The top panels show two representative oocytes containing the wild-type channel (left) and the Y1618K mutant channel (right), respectively. In the Y1618K mutant channel, the leftward shift of the inactivation curve by 100 μM lamotrigine (LMT), 100 μM phenytoin (DPH), or 300 μM carbamazepine (CBZ) is evidently smaller than that in the wild-type channel. Two sets of control data (control I and II, respectively; open symbols) were obtained before and after drug application in each plot to show no voltage drift during this long experiment. The lines are fits with a Boltzmann function. The averaged shift (ΔV) of the inactivation curve by 100 μM lamotrigine, phenytoin, or carbamazepine is shown in the bar graph ($n = 4$–5). **, $P < 0.05$ and ***, $P < 0.005$ by Student's t test (compared with the wild-type data with 100 μM carbamazepine).

Concomitant mutations of the S3-4 linker residues close to Y1618 rather than those far away in the intracellular inactivation machinery abolish the inactivation-slowing effect of carbamazepine on Y1618K

We next examined whether other residues in the D4S3-4 linker could also affect the local conformation of the anticonvulsant receptor. Except for those mutations involving Y1618, we did not find any other point mutations (e.g., E1616K, K1617A, and F1619K) in the S3-S4 linker to have the inactivation-slowing effect by carbamazepine (see the F1619K current shown in Fig. 7 B as an example). However, concomitant substitutions of the residues nearby Y1618 in the S3-S4 linker could completely abolish the effect of Y1618K mutation on the action of carbamazepine. For example, in the Y1618K/F1619K, Y1618K/K1617A, or Y1618K/E1616K double-mutant channels, carbamazepine can no longer slow the macroscopic inactivation (Fig. 7 B). Even a concomitant mutation (R1626C) at the outermost arginine of S4 (i.e., at the junction between the S3-4 linker and S4) also effectively wipes out the inactivation-slowing effect of carbamazepine on the Y1618K channel. On other hand, concomitant mutation at the presumable intracellular inactivation machinery, such as F1651A in the D4S4-5 linker (McPhee et al., 1998), well keeps the inactivation-slowing effect of carbamazepine made by Y1618K. In this

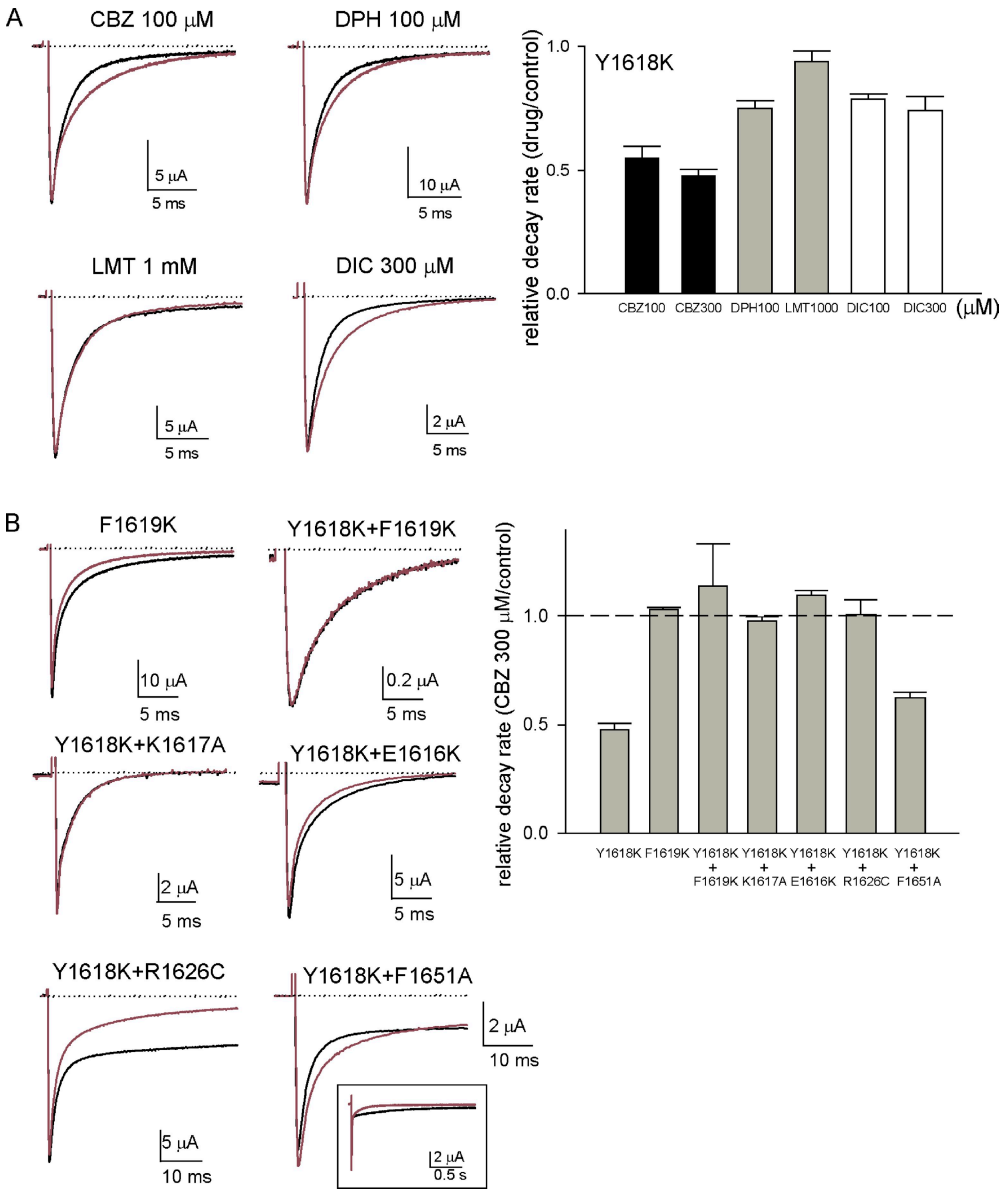

Figure 7. Delicate effects of drug structure and local conformation around Y1618 on the slowing of the macroscopic current decay in the Y1618K mutant channel. (A) The experiments and plots are done in the Y1618K mutant channel with the same methods described in Fig. 5, except that different concentrations of different anticonvulsants were applied. The macroscopic currents recorded in the presence (red lines) and absence (black lines) of drugs are superimposed. The slowing effects on the macroscopic current decay by 100 μM carbamazepine, 100 μM phenytoin, and 300 μM diclofenac are discernible. However, lamotrigine, even at 1 mM, only has a negligible effect on the decay. The dotted line indicates zero current level. The relative decay rates (the decay rate in drug relative to that in control) in the Y1618K mutant channel are shown in the bar graph for different concentrations of different drugs (n = 3–9). (B) The effect of concomitant mutations of another residue in the D4S3-4 linker or in the D4S4-5 linker on the slowed macroscopic current decay by carbamazepine in the Y1618K mutant channel. The macroscopic currents recorded in the presence (red lines) and absence (black lines) of 300 μM carbamazepine are superimposed. In the F1619K single-mutant and the Y1618K plus F1619K, K1617A, E1616K, or R1626 double-mutant channels, 300 μM carbamazepine shows no slowing effect on the macroscopic current decay. On the other hand, in the Y1618K/F1651A double-mutant channel, carbamazepine still slows the development of the partially impaired inactivation (ascribable to F1651A mutation). In this case, however, carbamazepine still helps to stabilize inactivation and reduces the sustained current at the end of a prolonged depolarizing pulse (e.g., 2 s; the inset figure). The dotted line indicates zero current level. (Right) The macroscopic decay rate in 300 μM carbamazepine is normalized to that in control to obtain the relative decay rate in different mutant channels (n = 3–9).

regard, it is especially noted that the apparent macroscopic currents are similar in the Y1618K/R1626C and Y1618K/F1651A double-mutant channels (both having partially impaired inactivation; see representative currents in Fig. 7 B). These findings further substantiate a very local effect of Y1618 mutation on the alteration of drug binding geometry. It is also notable in the Y1618K/F1651A double-mutant channel that, despite the slowed inactivation kinetics by carbamazepine, the drug still stabilizes the inactivation state that is partially impaired by F1651A (Fig. 7 B, inset).

Cd^{2+} and Zn^{2+} interaction with the Y1618H plus W1716H double mutation reveals close proximity between S3-4 linker and SS6 pore-lining segment in domain 4

We have argued that there is a delicate interaction between Y1618 in the S3-4 linker and the common anticonvulsant receptor presumably in the external pore mouth. We have also seen in Figs. 1–4 that W1716 very likely interacts with F1764 to be responsible for the drug receptor and proper ion permeation. To explore possible interaction between Y1618 and W1716, we initially made Y1618K/W1716E and Y1618C/W1716C double

mutations, but did not observe any discernible currents. We then took an alternative approach and introduced histidine substitutions for Y1618 and/or W1716. Fig. 8 shows the effect of externally applied group IIB divalent cations, namely Cd^{2+} and Zn^{2+}, on these mutant channels. The channel pore does not seem to be significantly blocked by 100–300 μM Cd^{2+} and Zn^{2+} in these mutant channels (e.g., slightly decreased peak current without evident acceleration of current decay by Cd^{2+} or Zn^{2+}). However, the macroscopic activation kinetics is significantly retarded by both Cd^{2+} and Zn^{2+} in the Y1618H/W1716H double mutant, but not in either component single-mutant channels (i.e., Y1618H or W1716H; Fig. 8 A). Moreover, the activation curve of the Y1618H/W1716H double-mutant (but not of either single-mutant) channel is dramatically shifted to the right on the voltage axis by Cd^{2+} and Zn^{2+} (Fig. 8 B). These findings indicate a metal-chelating site formed by close proximity of the two histidine residues. Also, because domain 4 is primarily considered a structure specialized for Na^+ channel inactivation, it is highly interesting that the binding of non-permeating divalent cations onto Y1618H/W1716H should dramatically affect channel activation (see below).

The altered gating curves and carbamazepine action suggest close proximity between Y1618 and L1719 in the pore loop

The findings in Fig. 8 suggest close proximity between Y1618 in the S3-4 linker and W1716 in the pore loop of domain 4. To investigate the other potential interactions between Y1618 and the external pore loop residues in domain 4, we did "glutamate screening" of the residues in the vicinity of W1716, i.e., those in the D4 pore loop external to the presumable selectivity filter residue (A1714 of the DEKA ring). With glutamate substitutions for the pore residues G1715 through L1720 (except D1717, which itself is a negatively charged residue and was therefore mutated to alanine), we found no significant changes in the activation and inactivation curves of these single-mutant channels (not depicted). However, when these glutamate substitutions are made with Y1618K, the inactivation curve is specifically shifted to the left by ~30 mV in the Y1618K/L1719E double-mutant channel, in contrast with a much smaller change in the activation curve (Fig. 9, A and B). To verify the electrostatic interaction between the countercharges, we did reverse mutations at Y1618 and L1719. There is no observable current

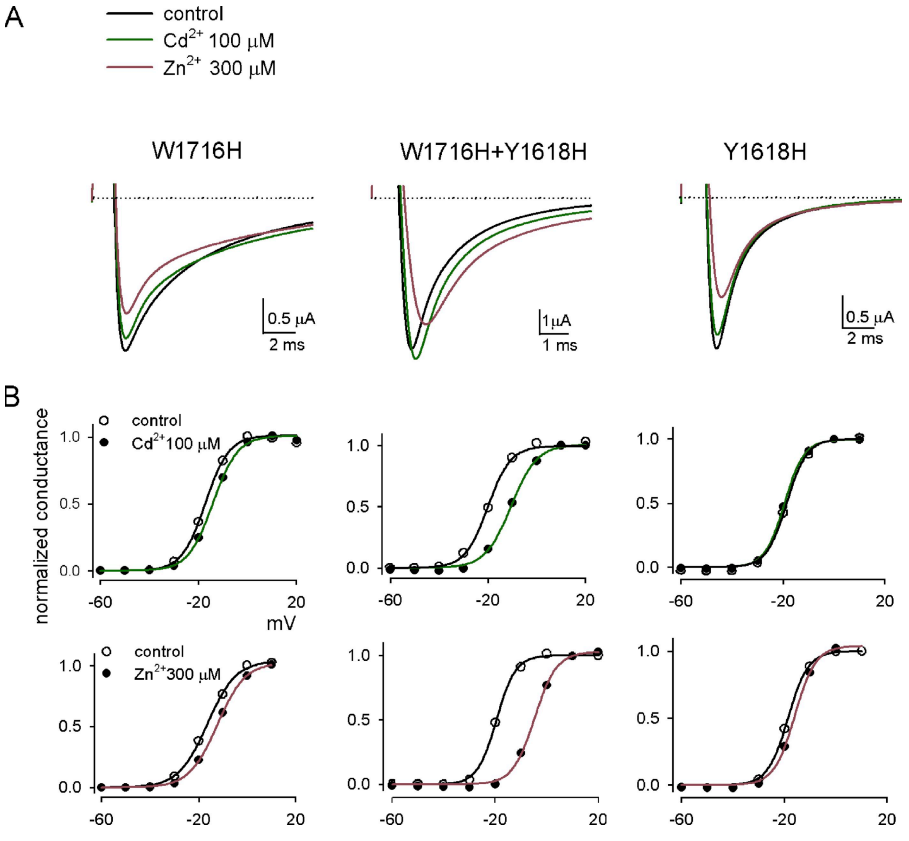

Figure 8. The effect of external group IIB divalent cations on the Y1618H, W1716H, and Y1618H plus W1716H mutant channels. (A) The representative currents in the absence (solid black lines) and presence of 100 μM Cd^{2+} (green lines) and 300 μM Zn^{2+} (red lines) on the same oocyte. The oocyte was held at −120 mV and stepped to −10 mV to elicit Na^+ currents. The pulse protocol was repeated every 3 s until a steady-state effect of Cd^{2+} or Zn^{2+} was reached. The effects of both Cd^{2+} and Zn^{2+} can be readily washed out with the control ND-96 solution, and the observed effect remains the same regardless of the order of Cd^{2+} and Zn^{2+} application. The dotted lines mark the zero current level. (B) The activation curves in the absence (open circles and solid black lines) and presence of 100 μM Cd^{2+} (top panels; closed circles and green lines) or 300 μM Zn^{2+} (bottom panels; closed circles and red lines) were done by the protocols described in Materials and methods. The lines are fits with a Boltzmann function with $V_{1/2}$ values (control vs. Cd^{2+}) in mV of −17.2 versus −14.2, −19.7 versus −10.6, and −18.6 versus −19.5, and k values (control vs. Cd^{2+}) of 4.8 versus 5.0, 4.9 versus 5.3, and 3.9 versus 3.8, and $V_{1/2}$ values (control vs. Zn^{2+}) in mV of −16.5 versus −12.4, −19.5 versus −4.7, and −18.6 versus −16.0, and k values (control vs. Zn^{2+}) of 5.9 versus 5.8, 3.7 versus 4.2, and 3.9 versus 4.0 for the W1716H, the Y1618H plus W1716H, and the Y1618H mutant channels, respectively. The averaged shift of the $V_{1/2}$ of the activation curve by Cd^{2+} is 0.8 ± 0.2, 1.9 ± 1.0, and 8.2 ± 0.9 mV, and the averaged $V_{1/2}$ shift by Zn^{2+} is 2.6 ± 1.1, 3.7 ± 2.0, and 10.7 ± 2.6 mV for the Y1618H, the W1716H, and the Y1618H plus W1716H mutant channels, respectively (n = 3–4).

from the Y1618E mutant channel, but the Y1618D/L1719K double mutation also has a prominent effect on the gating curves, very much similar to the case in the Y1618K/L1719E double mutation. It should be noted that not any corresponding component single mutation here (i.e., Y1618K, L1719E, Y1618D, and L1719K) has significant effect on the gating curves (not depicted). These findings are very much reminiscent of the consequence of the mutations at F1625 (located between the S3-4 linker and the S4), where stabilization of a presumably extruded D4S4 by different mutations results in stabilization of inactivation (e.g., a large-scale leftward shift of the inactivation curve) without alteration in channel activation (Yang and Kuo, 2003). The relatively long side chains of lysine and glutamate (or aspartate) in Y1618K/L1719E and Y1618D/L1719K probably interact to stabilize the D4S4 voltage sensor in an outwardly translocated position and consequently stabilize channel inactivation. If Y1618K differentially interacts with L1719E during S4 outward translocation, it would be interesting to see how the gating conformational changes in the anticonvulsant receptor are altered by the double mutation. We found that carbamazepine still retards the macroscopic inactivation rate in the Y1618K/L1719E double-mutant channel at 0 mV (Fig. 10, A and B). However, the Y1618K/L1719E double mutation abolishes the voltage dependence of the carbamazepine effect on the inactivation rate (Fig. 10 C). In the Y1618K single mutant as well as in Y1618K plus G1715E, G1718E, or L1720E (but not L1719E), double-mutant channels, when the membrane voltage becomes more depolarized, the inactivation slowing by carbamazepine is more prominent and the effect is then "saturated" at more positive voltages. This voltage-dependent and eventually saturated phenomenon may imply that the retarded D4S4 movement (which is critically associated with channel inactivation; Yang and Kuo, 2003) by carbamazepine would become more rate limiting in the whole macroscopic inactivation process (which is coupled to channel activation) at more depolarized membrane potentials. The lack of voltage dependence of the carbamazepine effect in the Y1618K/L1719E double-mutant channel thus suggests either significant uncoupling of inactivation from activation or additional retardation of channel activation by carbamazepine. The former does not seem to be the case because the voltage dependence of the macroscopic inactivation rates in the absence of carbamazepine remains very similar (i.e., becoming faster and saturating with more depolarized potentials such as −10 to 20 mV; Fig. 10 D) in all mutant channels, including Y1618K/L1719E. On the other hand, the latter seems plausible as we found that the activation curve is rightwardly shifted and the macroscopic activation is slowed by carbamazepine in the Y1618K/L1719E double-mutant channel (Fig. 10 E; note that there is no discernible change in activation of the Y1618K single-mutant channel; not depicted). This is consistent with the findings in Fig. 8, where the binding of external ligands and presumably a subsequent connection between the D4S3-4 linker and the pore loop would slow the macroscopic activation rate and shift the activation curve. This prominent action of carbamazepine on channel activation is also consistent with the idea of significant binding of carbamazepine to the resting Y1618K mutant channel. It is plausible that the altered interaction between the D4S3-4 linker and D4 pore loop may allow a partially extruded D4S4 position (Fig. 9) even in the "resting" channel, to which carbamazepine may bind to retard

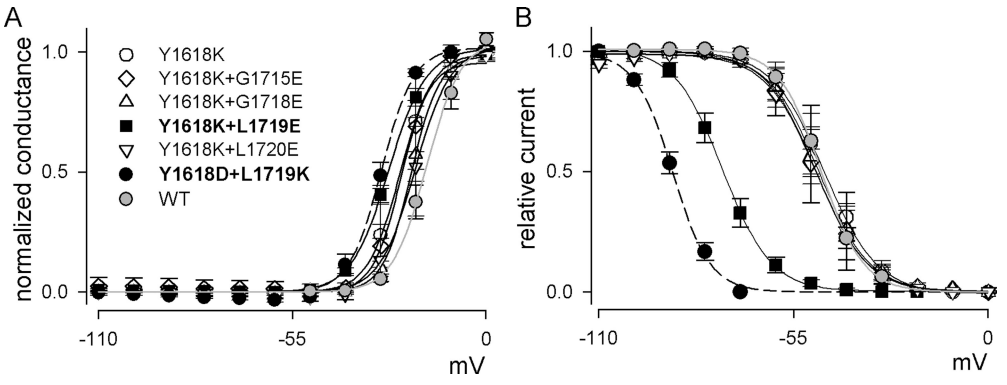

Figure 9. Alterations in the activation and inactivation curves by the interaction between the countercharges introduced to Y1618 and the pore loop residues in domain 4. The averaged activation curves (A) and inactivation curves (B; the inactivating pulse duration = 100 ms) were done by the protocols described in Materials and methods (n = 3–5). The lines in the left panel are fits with a Boltzmann function with $V_{1/2}$ values (in mV) of −24.5, −23.4, −21.4, −27.7, −20.5, and −29.7, and k values of 4.6, 4.2, 4.0, 5.2, 5.2, and 4.6 for Y1618K, Y1618K plus G1715E, Y1618K plus G1718E, Y1618K plus L1719E, Y1618K plus L1720E, and Y1618D plus L1719K mutant channels, respectively. The data for the wild-type channel are from Fig. 1 A. The lines in the right panel are fits with a Boltzmann function with $V_{1/2}$ values (in mV) of −47.2, −46.1, −48.6, −47.8, −75.0, −48.5, and −89.1, and k values of 6.0, 7.3, 6.9, 6.8, 6.7, 7.0, and 5.3 for the wild-type, 1618K, Y1618K plus G1715E, Y1618K plus G1718E, Y1618K plus L1719E, Y1618K plus L1720E, and Y1618D plus L1719K mutant channels, respectively. We also did the inactivation curves with 9-s inactivating pulses and found that the inactivation curve is still leftward shifted by ∼30 mV in the Y1618K/L1719E double-mutant channel compared with the wild-type channel. The data for the wild-type channel are shown as gray circles with gray lines.

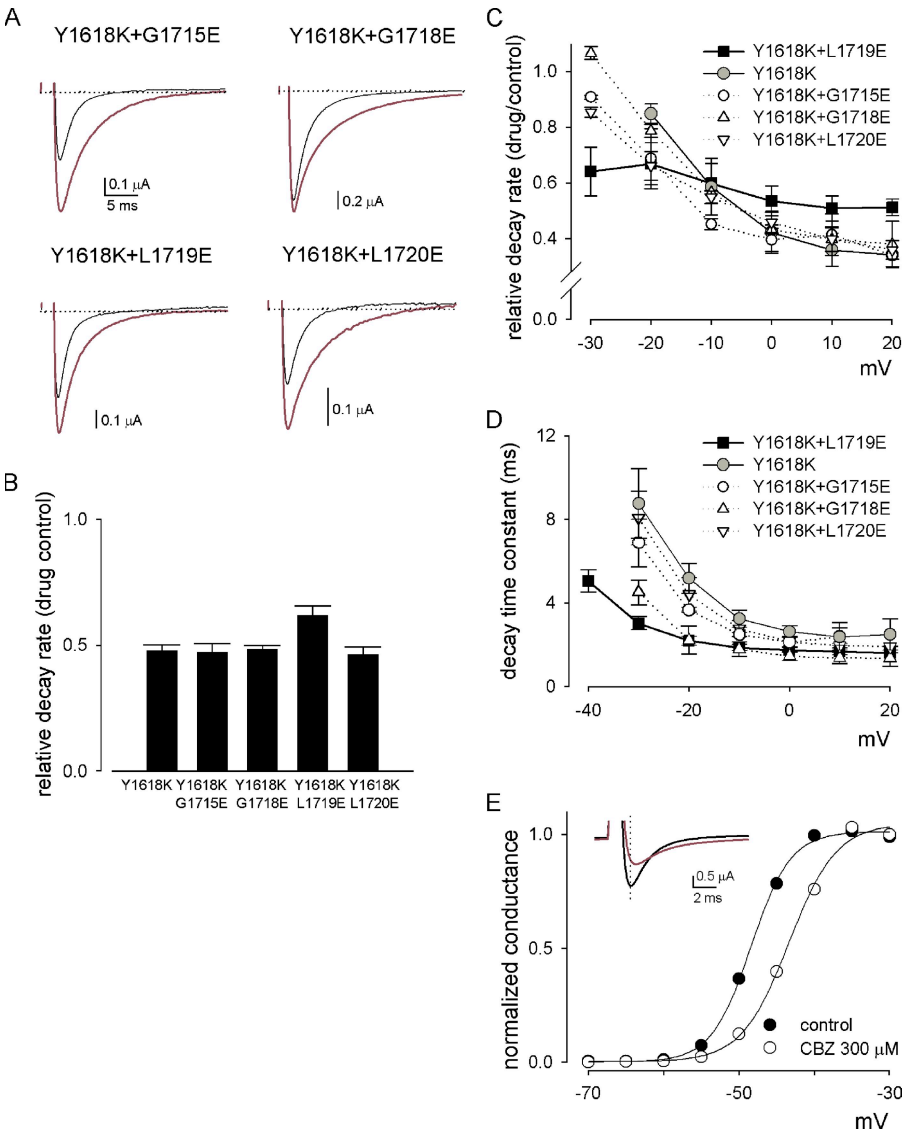

Figure 10. Carbamazepine action on the mutant channels containing Y1618K and glutamate substitutions for the pore loop residues in domain 4. (A) The two superimposed traces show the representative currents elicited from a holding potential of −120 mV to a test depolarization at 0 mV in the absence (black lines) and presence (red lines) of 300 μM carbamazepine. The dotted line indicates zero current level. (B) The macroscopic current decays in A are quantified by the methods in Fig. 1 D to give the relative decay rates for different mutant channels (n = 3–4). (C) The relative decay rates of the macroscopic currents (in 300 μM carbamazepine vs. in control) are examined at different test voltages and in different mutant channels (n = 3–4 for each different channel). Note the apparent lack of voltage dependence of the data from the Y1618K/L1719E double-mutant channel. (D) The decay time constants (in ms) of the macroscopic currents in control (i.e., without any drug) are plotted against different test voltages in different mutant channels (n = 4 for each different channel). The mutant channels in the figure all have significantly faster saturating inactivation kinetics than the wild-type channel. The decay time constants examined at +10 mV for the mutant channels are all ranged between 1.4 ± 0.26 and 2.4 ± 0.41 ms, and that for the wild-type channel (n = 9) is 4.1 ± 0.83 ms ($P < 0.001$ between any one mutant channel and the wild-type channel compared by Student's t test). (E) Carbamazepine alters activation of the Y1618K plus L1719E double-mutant channel. The activation curves of the mutant channel were done by the protocols described in Materials and methods. The lines are fits of the data from the same oocyte with a Boltzmann function with $V_{1/2}$ values (in mV) of −26.9 and −16.8, and k values of 5.1 and 6.1 in the absence (black circles) and presence (white circles) of 300 μM carbamazepine. The averaged shift of the $V_{1/2}$ of the activation curve by 300 μM carbamazepine is 7.2 ± 2.6 mV (n = 3). The inset contains representative currents elicited by a step depolarization to −20 mV from a holding potential of −120 mV. The dotted vertical line marks the time point when the peak macroscopic current in control (black line) is reached. It is evident that 300 μM carbamazepine (red line) slows the macroscopic activation (rightward shifts the peak of macroscopic current) of the Y1618K plus L1719E mutant channel.

(in terms of a kinetic rather than a steady-state effect) further movement of D4S4 and thus the occurrence of channel inactivation. The capability of carbamazepine binding to the resting mutant channel to retard channel activation, together with the incapability of the bound carbamazepine to block the mutant channel pore, indicates that the interaction between D4S3-4 linker and D4 pore loop is a critical pivotal point between channel gating and ion permeation, very likely playing an imperative role in both the state-dependent conformational changes in the anticonvulsant receptor and the activation-inactivation coupling.

DISCUSSION

W1716 in the external pore loop is located in close proximity to F1764 in the internal part of S6 in domain 4 of the Na^+ channel

Two aromatic residues, W1716 and F1764, have been reported to contribute to anticonvulsant binding to the Na^+ channel (Ragsdale et al., 1994, 1996; Tsang et al., 2005; McNulty et al., 2007). In this study, we demonstrate that W1716 (in the external pore loop) is located in close proximity to F1764 (presumably lining the internal compartment of the pore of the S6 helix). First,

in terms of the effect on carbamazepine binding affinity, the non-additive feature of W1716 and F1764 mutations suggests that the two residues do not independently contribute to the drug receptor. Moreover, the estimated interaction energy between W1716 and F1764 falls into the range expected for two closely spaced interacting aromatic side chains in a protein (Table I) (Serrano et al., 1991; Smith and Regan, 1995; Tatko and Waters, 2002; Hong et al., 2007). Second, F1764C reduces channel inactivation that is enhanced by W1716C and abolishes the accessibility of W1716C to the external MTSET, MTSES, and Cd^{2+}. Third, the ion selectivity for Na^+ over K^+ of the W1716E mutant is abolished by introducing a countercharge at F1764 (i.e., F1764R). Fourth, double mutation of F1764R and G1715E (and also F1764R and L1719E) causes a large shift in the activation curve (but G1715E, L1719E, or F1764R single mutation does not have such an effect). These findings give rise to novel structural insight that the external pore-lining segment SS6 is located very close to the internal pore compartment of S6, enabling an alternative connection bypassing the selectivity filter between the external and internal compartments of the Na^+ channel pore. This alternative connection can be reasonably conceived because there must be a turn between the SS6 (the carboxyl end) of the pore loop and the S6 helix (Fig. 11). In this regard, the S6 helix in the vicinity of F1764 may form a "recess" of the pore, so that the side chain at this F1764 position could present itself beside the SS6 pore loop to face the external part of the pore without trespassing the selectivity filter.

The "S6 recess" connects the internal and external vestibule of the channel pore: a revision of the pore configuration and the hydrophobic pathway of drug action

We have proposed that the external and internal parts of the pore might be connected by not only a narrow selectivity filter in the pore, but also an interacting common "wall" between the "S6 recess" and the external pore mouth (Fig. 11). For the travelers bearing high charge density and significant inner hydration shell, such as metal ions, the only pathway through the pore is via the narrow selectivity filter that is equipped with coordinating ligands arranged in appropriate spatial configuration to replace the water molecules in the hydration shell. On the other hand, drug molecules that are uncharged or with lower charge density may interact with the common wall between the external and internal parts of the pore, or even "sneak" across it. For instance, internal and external QX-314, a charged molecule with much lower charge density than inorganic ions, may both bind to the very "same" site in the pore, and then exit to the other side of the pore without traveling through the selectivity filter. S6 recess thus would provide not only an innovative idea of the versatile demarcation between the "internal" and "external" parts of the channel pore traditionally linked by the selectivity filter, but also a more specific physical picture accounting for the classical proposal of a "hydrophobic pathway" for local anesthetic binding to the Na^+ channel (Hille, 1977; see also Zhang et al., 2007). In this regard, it is notable that F1764 is also involved in the binding site of batrachotoxin (Linford et al., 1998; Wang and Wang, 1999). Batrachotoxin is a lipid-soluble alkaloid neurotoxin and a specific Na^+ channel activator. The batrachotoxin binding site has been located in the domain "interface" chiefly involving D1S6 and D4S6 rather than in the main ion conduction pathway (Zamponi and French, 1994; Wang and Wang, 1999; De Leon and Ragsdale, 2003). With the idea of S6 recess, batrachotoxin binding to F1764 thus may not block the channel pore (because it is in the S6 recess), but may alter ion selectivity (due to the altered W1716–F1764 interaction; see Fig. 3). This is also reminiscent of the recent finding that charges at the position equivalent to 1764 affect permeation in human cardiac $Na_v1.5$ (McNulty et al., 2007). The S6 recess also well explains the apparently perplexing finding that V1583C in skeletal Na^+ channels (equivalent to V1768 in $Na_v1.2$ channels) could be modified by either internal or external MTESA, and that the modification is blocked by batrachotoxin but not 20 mM of the internal pore-blocking tetraethylammonium (Vedantham and Cannon, 2000). Together with the intriguing findings that I1760A but not I1760C makes the channel more sensitive to external Cd^{2+} block (Wang et al., 1998; Sunami et al., 2001), it seems plausible that the series of residues I1760-F1764-V1768 may line a recess that is directly connected to the internal vestibule of the pore but are also intimately associated with the external vestibule of the channel pore. Aromatic side chains are suggested to be critical for the proper folding and positioning of integral membrane proteins in the lipid bilayer because they are found enriched at the membrane–water interface and render the highest tendency to partition into the membrane–water interface (Wimley and White, 1996; Killian and von Heijne, 2000; Hessa et al., 2005). By the same token, W1716 and F1764 may build up and stabilize a recess at an interface between the hydrophobic element, such as lipid bilayer and the hydrophilic path, that the permeating ions can actually travel through.

Membrane depolarization moves the S3-4 linker close to the pore loop in domain 4 to shape the anticonvulsant receptor in the external pore mouth

In Fig. 5 we show that a point mutation Y1618K in D4S3-4 linker makes the Na^+ channel inactivation kinetics evidently slowed by carbamazepine. This finding not only indicates that carbamazepine is turned into an ineffective pore blocker by the mutation, but also is very much reminiscent of the inactivation-deterring effect of external multivalent transitional pore-blocking

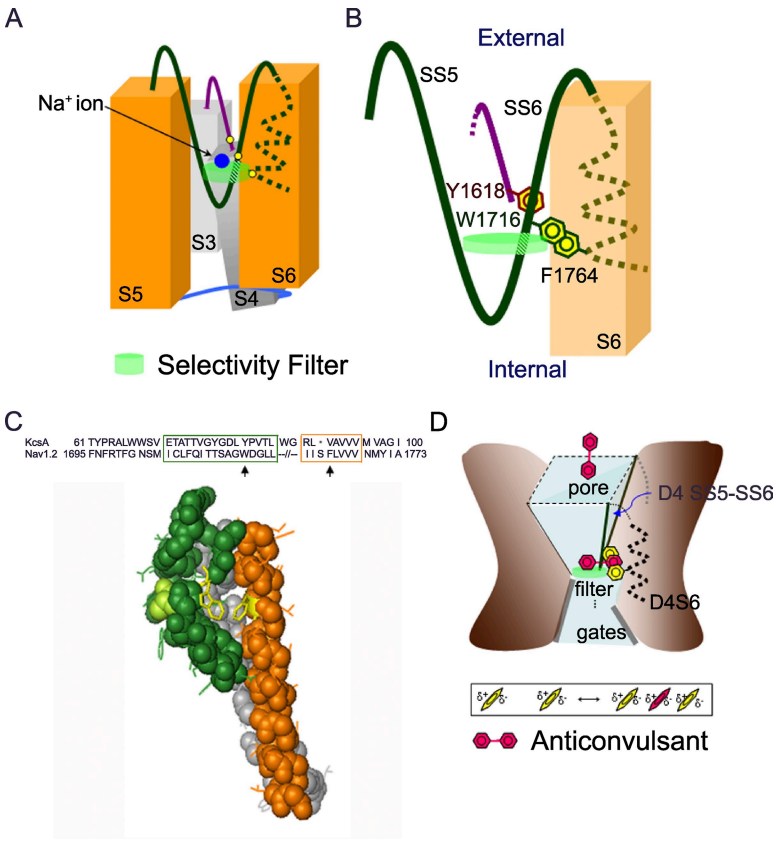

Figure 11. A model illustrating the close proximity and interactions among the S3-4 linker (e.g., Y1618), the SS6 pore loop (e.g., W1716), and the internal pore-lining part of S6 (e.g., F1764) in domain 4 of the Na^+ channel, making a pivotal apparatus for ion permeation, activation-inactivation coupling, and drug binding. (A) The transmembrane segments S3–S6 in domain 4 of the channel are plotted as rectangular cylinders and viewed from the pore. W1716 is adjacent to A1714 in sequence, and thus is most likely located externally to the selectivity filter in the SS6 pore loop. This position could reasonably interact with F1764 of S6 if there is a turn at the junction of SS6 loop and S6 helix. As a result, the S6 helix in the vicinity of F1764 forms a "recess" of the pore. The aromatic residues Y1618, W1716, and F1764 are plotted as yellow dots. Membrane voltage changes move the S4 segment, and thus move the S3-4, S4-5, and S5-6 linkers to contribute to the essential voltage-dependent physiological and pharmacological attributes of the channel. (B) An enlarged picture for the interacting aromatic residues in A. (C) A homology model for the S6 recess of domain 4 in Nav1.2 based on the crystallized structure of the KcsA K^+ channel pore (done by an online server provided by the Swiss Institute of Bioinformatics: http://swissmodel.expasy.org). Because of the marked difference in the length of the pore loops between these two types of channels, the homology modeling is based on somewhat arbitrary sequence alignment of the key conservative residues of D4SS6 and S6 (marked by green and orange rectangles, respectively) in the $Na_v1.2$ channel and a subunit in the KcsA channel, with a large portion of pore loop in Nav1.2 deleted (top panel; note the sequence numbering and the arrows indicating W1716 and F1764). In the molecular model (bottom panel), the S5, S6, and S5-S6 linker of domain 4 are shown as space fills and colored gray, orange, and dark green, respectively. A1714 is in light green to mark the possible location of the selectivity filter. The aromatic side chains of W1716 in SS6 and F1764 in S6 are shown in yellow. A carbamazepine molecule could be well docked to a receptor constituted by W1716 and F1764 in the recess region of this model with the Discovery Studio software (Accelyrs Inc.; not depicted). (D) The brown-colored areas illustrate the other part of the channel protein surrounding the aqueous pore region (light blue), which is made by the four SS5-SS6 loops from the four domains (illustrated as the four "walls" making the external part of the pore). W1716 on the SS5-SS6 loop and F1764 on S6 (dotted helix; both residues depicted as yellow phenyl groups) of domain 4 interact to form a recess, which is more readily depicted with an angle of view roughly perpendicular to that in A and B. The anticonvulsant drug (shown as a pink diphenyl motif) presumably binds to its receptor located at the S6 recess with dipole-induced dipole interactions among the phenyl groups of the drug (pink), W1716 and F1764 (both in yellow; the boxed picture). A hydrophobic drug molecule of suitable conformation could even go through the S6 recess and thus traverse the pore without trespassing on the selectivity filter, embodying the long-proposed "hydrophobic" pathway of local anesthetic action on the Na^+ channel.

metal ions (Kuo et al., 2004) or α-scorpion toxins (site-3 neurotoxins; Tejedor and Catterall, 1988; Thomsen and Catterall, 1989; Rogers et al., 1996; Benzinger et al., 1998). In this regard, it is interesting to note that although carbamazepine, phenytoin, and lamotrigine bind to an external common anticonvulsant receptor with a structurally similar dephenyl motif (Kuo, 1998a; Kuo et al., 2000), they do have a very different inactivation-slowing effect in the Y1618K channel (Fig. 7 A). Moreover, many concomitant point mutations in the adjacent (but not more distant) areas in the D4S3-4 linker and D4S4 abolish the inactivation-slowing effect of carbamazepine with Y1618K. The inactivation-deterring effect is thus very likely ascribable to a delicate and local conformational change (rather than a long-range allosteric interaction). In addition, the direct interaction between the external S3-4 linker and the pore loop (e.g., via the double mutant of Y1618K plus L1719E) could alter the action of carbamazepine on gating kinetics while keeping the gating kinetics relatively unchanged in the absence of the drug (Fig. 10, C–E). The effect of external Y1618K-L1719E interaction thus is most likely ascribable to a truly local mechanism rather than an allosteric mechanism due to gating alteration. Collectively, the anticonvulsant receptor should be intimately related to the D4S3-4 linker and the D4 pore loop, and thus it directly involves the external region of the Na^+ channel pore. Consistently, site-3 neurotoxins were shown to bind to the D4S3-4 linker and the pore loops of domains 1 and 4 to slow Na^+ channel inactivation (Tejedor and Catterall, 1988; Thomsen and Catterall, 1989; Rogers et al., 1996;

Benzinger et al., 1998). The findings that concomitant mutations in the D4S3-4 linker and in D4S4 may decrease or abolish the effect of each other on carbamazepine action or channel inactivation (Fig. 7 B) (Yang and Kuo, 2003), and that site-3 neurotoxins seem to inhibit gating currents associated with the movement of D4S4 (Sheets et al., 1999), all strongly support a tight control of the D4S3-4 linker on the movement of D4S4. There have been different kinds of instances suggesting significant gating-permeation coupling on the extracellular side of Na^+ channels (e.g., Tomaselli et al., 1995; Hilber et al., 2001; Kuo et al., 2004). There are even more reports on the closeness or significant interaction between the gating voltage sensor and the pore domain in the Shaker K^+ channel (e.g., Li-Smerin and Swartz, 2000; Elinder et al., 2001; Gandhi et al., 2003; Laine et al., 2003). The interaction between the D4S3-4 linker and the pore loop in domain 4 may well constitute a pivotal point coupling channel gating to ion permeation in addition to the classical role played by the intracellular gates of the Na^+ channel (West et al., 1992; McPhee et al., 1998; Motoike et al., 2004; Popa et al., 2004).

The external pore loop in domain 4 is probably a pivotal point coupling not only gating and permeation, but also activation and inactivation of the Na^+ channel

The fourth domain (D4) of the Na^+ channel has been viewed as a structure specialized for inactivation. D4S4 is specifically responsible for channel inactivation rather than activation (Stühmer et al., 1989; Chahine et al., 1994; Chen et al., 1996; Kühn and Greeff, 1999; Sheets et al., 1999; Yang and Kuo, 2003). In addition, the D4S4-S5 linker, the intracellular part of D4S6, and the D3-4 linker (functionally the amino terminus of D4) presumably constitute the major parts of the Na^+ channel inactivation machinery (McPhee et al., 1995, 1998). In this regard, it is intriguing that channel activation could be specifically altered in the D4S3-4 linker and D4 pore loop double mutations (Figs. 8 and 10). Moreover, the G1715E/F1764R double mutation leads to a dramatic right shift in the activation curve but does not alter the inactivation curve. This is reminiscent of the finding that the selectivity filter residue in domain 4 undergoes conformational changes during channel activation (Hilber et al., 2001). It has been shown that the pore loops from different domains may have intimate interactions. For example, double mutations comprised of G1530C in the domain 4 pore loop and Y401C in the domain 1 pore loop create a high-affinity binding site for Cd^{2+} in the μ1 Na^+ channel (Béinitah et al., 1996). Together with the pore loop–pore loop interaction, the S3-4 linker–pore loop interaction may then serve to couple S4 movement in different domains. The very selective or polarized effect of mutations in the D4 external pore region on either channel activation or inactivation presumably indicates specific conformations (of the D4 external pore region) permissive for either channel activation or inactivation, or, very likely, permissive for the S4 movement in one domain but not in the other. Channel activation then could give rise to specific "intermediate" conformational changes in the D4 external pore region. These changes are deemed intermediate because they could not yet affect the occurrence of channel inactivation or the movement of D4S4. In summary, it seems plausible that the moving S4 upon membrane voltage changes has significant interactions with the pore domain on both ends. Those interactions on the intracellular side may involve the S4-5 linker (e.g., McPhee et al., 1998) to "pull" on the more carbonyl-end part of S6, where the activation/inactivation gates are presumably located. In contrast, the interactions on the extracellular side are most likely relayed from the voltage sensor to the external pore loop via the S3-4 linker, and are responsible for the stepwise conformational changes closely related to activation-inactivation coupling. The interactions on the two ends may finally merge at or near the S6 recess. The inner part of the external vestibule of the Na^+ channel pore may therefore not only have a critical function in ion permeation by constituting the selectivity filter of the channel, but also serve as a pivotal point transducing and coordinating the essential gating conformational changes. This could be the reason why this part of the Na^+ channel also makes an ideal receptor site for many important gating-modifying and/or pore-blocking drugs and neurotoxins.

We thank Sin Lin and Yu-Dien Chen for technical assistance.

This work was supported by the National Science Council, Taiwan (grant NSC97-2320-B-002-039-MY3 to C.-C. Kuo and grant NSC97-2311-B-182-005-MY2 to Y.-C. Yang), and by the National Health Research Institutes, Taiwan (grant NHRI-EX98-9606NI to C.-C. Kuo).

Lawrence G. Palmer served as editor.

Submitted: 13 November 2008
Accepted: 2 July 2009

REFERENCES

Bean, B.P. 1984. Nitrendipine block of cardiac calcium channels: high-affinity binding to the inactivated state. *Proc. Natl. Acad. Sci. USA.* 81:6388–6392.

Bean, B.P., C.J. Cohen, and R.W. Tsien. 1983. Lidocaine block of cardiac sodium channels. *J. Gen. Physiol.* 81:613–642.

Béinitah, J.-P., G.F. Tomaselli, and E. Marban. 1996. Adjacent pore-lining residues within sodium channels identified by paired cysteine mutagenesis. *Proc. Natl. Acad. Sci. USA.* 93:7392–7396.

Benzinger, G.R., J.W. Kyle, K.M. Blumenthal, and D.A. Hanck. 1998. A specific interaction between the cardiac sodium channel and site-3 toxin anthopleurin B. *J. Biol. Chem.* 273:80–84.

Butterworth, J.F., and G.R. Strichartz. 1990. Molecular mechanisms of local anesthesia: a review. *Anesthesiology.* 72:711–734.

Carter, P.J., G. Winter, A.J. Wilkinson, and A.R. Fersht. 1984. The use of double mutants to detect structural changes in the active site of the tyrosyl-tRNA synthetase (Bacillus stearothermophilus). *Cell.* 38:835–840.

Chahine, M., A.L. George, M. Zhou, S.J.W. Sun, R.L. Barchi, and R. Horn. 1994. Sodium channel mutations in paramyotonia congenita uncouple inactivation from activation. *Neuron.* 12:281–294.

Chen, L.-Q., V. Santarelli, R. Horn, and R.G. Kallen. 1996. A unique role for the S4 segment of domain 4 in the inactivation of sodium channels. *J. Gen. Physiol.* 108:549–556.

Cohen, L., N. Ilan, M. Gur, W. Stühmer, D. Gordon, and M. Gurevitz. 2007. Design of a specific activator for skeletal muscle sodium channels uncovers channel architecture. *J. Biol. Chem.* 282:29424–29430.

Courtney, K.R., J.J. Kendig, and E.N. Cohen. 1978. The rate of interaction of local anesthetics with sodium channels in nerve. *J. Pharmacol. Exp. Ther.* 207:594–604.

De Leon, L., and D.S. Ragsdale. 2003. State-dependent access to the batrachotoxin receptor on the sodium channel. *Neuroreport.* 14:1353–1356.

Elinder, F., R. Mannikko, and H.P. Larsson. 2001. S4 charges move close to residues in the pore domain during activation of a K^+ channel. *J. Gen. Physiol.* 118:1–10.

Gandhi, C.S., E. Clark, E. Loots, A. Pralle, and Y. Isacoff. 2003. The orientation and molecular movement of a K^+ channel voltage-sensing domain. *Neuron.* 40:515–525.

Hessa, T., H. Kim, K. Bihlmaier, C. Lundin, J. Boekel, H. Andersson, I. Nilsson, S.H. White, and G. von Heijne. 2005. Recognition of transmembrane helices by the endoplasmic reticulum translocon. *Nature.* 433:377–381.

Hilber, K., W. Sandtner, O. Kudlacek, I.W. Glaaser, E. Weisz, J.W. Kyle, R.J. French, H.A. Fozzard, S.C. Dudley, and H. Todt. 2001. The selectivity filter of the voltage-gated sodium channel is involved in channel activation. *J. Biol. Chem.* 276:27831–27839.

Hille, B. 1977. Local anesthetics: hydrophilic and hydrophobic pathways for the drug-receptor reaction. *J. Gen. Physiol.* 69:497–515.

Hong, H., S. Park, R.H.F. Jiménez, D. Rinehart, and L.K. Tamm. 2007. Role of aromatic side chains in the folding and thermodynamic stability of integral membrane proteins. *J. Am. Chem. Soc.* 129:8320–8327.

Killian, J.A., and G. von Heijne. 2000. How proteins adapt to a membrane–water interface. *Trends Biochem. Sci.* 25:429–434.

Kühn, F.J.P., and N.G. Greeff. 1999. Movement of voltage sensor S4 in domain 4 is tightly coupled to sodium channel fast inactivation and gating charge immobilization. *J. Gen. Physiol.* 114:167–183.

Kuo, C.-C. 1998a. A common anticonvulsant binding site for phenytoin, carbamazepine, and lamotrigine in neuronal Na^+ channels. *Mol. Pharmacol.* 54:712–721.

Kuo, C.-C. 1998b. Imipramine inhibition of transient K^+ current: an open-channel blocker preventing fast inactivation. *Biophys. J.* 75:2845–2857.

Kuo, C.-C., and B.P. Bean. 1994. Slow binding of phenytoin to inactivated sodium channels in rat hippocampal neurons. *Mol. Pharmacol.* 46:716–725.

Kuo, C.-C., and L. Lu. 1997. Characterization of lamotrigine inhibition of Na^+ channels in rat hippocampal neurons. *Br. J. Pharmacol.* 121:1231–1238.

Kuo, C.-C., R.-S. Chen, L. Lu, and R.-C. Chen. 1997. Carbamazepine inhibition of neuronal Na^+ currents: quantitative distinction from phenytoin and possible therapeutic implications. *Mol. Pharmacol.* 51:1077–1083.

Kuo, C.-C., B.-S. Lou, and R.-C. Huang. 2000. Inhibition of Na^+ current by diphenhydramine and other diphenyl compounds: molecular determinants of selective binding to the inactivated channels. *Mol. Pharmacol.* 57:135–143.

Kuo, C.-C., W.-Y. Chen, and Y.-C. Yang. 2004. Block of tetrodotoxin-resistant Na^+ channel pore by multivalent cations: gating modification and Na^+ flow dependence. *J. Gen. Physiol.* 124:27–42.

Laine, M., M.-C.A. Lin, J.P.A. Bannister, W.R. Silverman, A.F. Mock, B. Roux, and D.M. Papazian. 2003. Atomic proximity between S4 segment and pore domain in Shaker potassium channels. *Neuron.* 39:467–481.

Lang, D.E., C.M. Wang, and B.R. Cooper. 1993. Lamotrigine, phenytoin and carbamazepine interactions on the sodium current present in N4TG1 mouse neuroblastoma cells. *J. Pharmacol. Exp. Ther.* 266:829–835.

Lee, P.J., A. Sunami, and H.A. Fozzard. 2001. Cardiac-specific external paths for lidocaine, defined by isoform-specific residues, accelerate recovery from use-dependent block. *Circ. Res.* 89:1014–1021.

Linford, N.J., A.R. Cantrell, Y. Qu, T. Scheuer, and W.A. Catterall. 1998. Interaction of batrachotoxin with the local anesthetic receptor site in transmembrane segment IVS6 of the voltage-gated sodium channel. *Proc. Natl. Acad. Sci. USA.* 95:13947–13952.

Lipicky, R.J., D.J. Gilbert, and I.M. Stillman. 1972. Diphenylhydantoin inhibition of sodium conductance in squid giant axon. *Proc. Natl. Acad. Sci. USA.* 69:1758–1760.

Li-Smerin, Y., and K.J. Swartz. 2000. Localization and molecular determinants of the Hanatoxin receptors on the voltage-sensing domains of a K^+ channel. *J. Gen. Physiol.* 115:673–684.

Long, S.B., E.B. Campbell, and R. MacKinnon. 2005a. Crystal structure of a mammalian voltage-dependent Shaker family K^+ channels. *Science.* 309:897–903.

Long, S.B., E.B. Campbell, and R. MacKinnon. 2005b. Voltage sensor of Kv1.2: structural basis of electromechanical coupling. *Science.* 309:903–908.

Matsuki, N., F.N. Quandt, E.R.E. Ten, and J.Z. Yeh. 1984. Characterization of the block of sodium channels by phenytoin in mouse neuroblastoma cells. *J. Pharmacol. Exp. Ther.* 228:523–530.

McNulty, M.M., G.B. Edgerton, R.D. Shah, D.A. Hanck, H.A. Fozzard, and G.M. Lipkind. 2007. Charge at the lidocaine binding site residue Phe-1759 affects permeation in human cardiac voltage-gated sodium channels. *J. Physiol.* 581:741–755.

McPhee, J.C., D.S. Ragsdale, T. Scheuer, and W.A. Catterall. 1995. A critical role for transmembrane segment IVS6 of the sodium channel α-subunit in fast inactivation. *J. Biol. Chem.* 270:12025–12034.

McPhee, J.C., D.S. Ragsdale, T. Scheuer, and W.A. Catterall. 1998. A critical role of the S4-S5 intracellular loop in domain IV of the sodium channel α-subunit in fast inactivation. *J. Biol. Chem.* 273:1121–1129.

Motoike, H.K., H. Liu, I.W. Glaaser, A.-S. Yang, M. Tateyama, and R.S. Kass. 2004. The Na^+ channel inactivation gate is a molecular complex: a novel role of the COOH-terminal domain. *J. Gen. Physiol.* 123:155–165.

Popa, M.O., A.K. Alekov, S. Bail, F. Lehmann-Horn, and H. Lerche. 2004. Cooperative effect of S4-5 loops in domains D3 and D4 on fast inactivation of the Na^+ channel. *J. Physiol.* 561:39–51.

Qu, Y., J. Rogers, T. Tanada, T. Scheuer, and W.A. Catterall. 1995. Molecular determinants of drug access to the receptor site for antiarrhythmic drugs in the cardiac Na^+ channel. *Proc. Natl. Acad. Sci. USA.* 92:11839–11843.

Ragsdale, D.S., J.C. Mcphee, T. Scheuer, and W.A. Catterall. 1994. Molecular determinants of state-dependent block of Na^+ channels by local anesthetics. *Science.* 265:1724–1728.

Ragsdale, D.S., J.C. Mcphee, T. Scheuer, and W.A. Catterall. 1996. Common molecular determinants of local anesthetic, antiarrhythmic, and anticonvulsant block of voltage-gated Na^+ channels. *Proc. Natl. Acad. Sci. USA.* 93:9270–9275.

Riddall, D.R., M.J. Leach, and J. Garthwaite. 2006. A novel drug binding site on voltage-gated sodium channels in rat brain. *Mol. Pharmacol.* 69:278–287.

Rogers, J.C., Y. Qu, T.N. Tanada, T. Scheuer, and W.A. Catterall. 1996. Molecular determinants of high affinity binding of alpha-scorpion toxin and sea anemone toxin in the S3-S4 extracellular

loop in domain IV of the Na^+ channel alpha subunit. *J. Biol. Chem.* 271:15950–15962.

Schwartz, J.R., and G. Grigat. 1989. Phenytoin and carbamazepine: potential and frequency-dependent block of Na^+ currents in mammalian myelinated nerve fibers. *Epilepsia.* 30:286–294.

Serrano, L., M. Bycroft, and A.R. Fersht. 1991. Aromatic-aromatic interactions and protein stability. Investigation by double-mutant cycles. *J. Mol. Biol.* 218:465–475.

Sheets, M.F., J.W. Kyle, R.G. Kallen, and D.A. Hanck. 1999. The Na^+ channel voltage sensor associated with inactivation is localized to the external charged residues of domain IV, S4. *Biophys. J.* 77:747–757.

Smith, C.K., and L. Regan. 1995. Guidelines for protein design: the energetics of β sheet side chain interactions. *Science.* 270:980–982.

Stühmer, W., F. Conti, H. Suzuki, X.D. Wang, M. Noda, N. Yahagi, H. Kubo, and S. Numa. 1989. Structural parts involved in activation and inactivation of the sodium channel. *Nature.* 339:597–603.

Sunami, A., I.W. Glaaser, and H.A. Fozzard. 2001. Structural and gating changes of the sodium channel induced by mutation of a residue in the upper third of IVS6, creating an external access path for local anesthetics. *Mol. Pharmacol.* 59:684–691.

Sunami, A., A. Tracey, I.W. Glaaser, G.M. Lipkind, D.A. Hanck, and H.A. Fozzard. 2004. Accessibility of mid-segment domain IV S6 residues of the voltage-gated Na^+ channel to methanethiosulfonate reagents. *J. Physiol.* 561:403–413.

Tang, L., R.G. Kallen, and R. Horn. 1996. Role of an S4-S5 linker in sodium channel inactivation probed by mutagenesis and a peptide blocker. *J. Gen. Physiol.* 108:89–104.

Tatko, C.D., and M.L. Waters. 2002. Selective aromatic interactions in β-hairpin peptides. *J. Am. Chem. Soc.* 124:9372–9373.

Tejedor, F.J., and W.A. Catterall. 1988. A site of covalent attachment of alpha-scorpion toxin derivativesin domain I of the sodium channel alpha subunit. *Proc. Natl. Acad. Sci. USA.* 85:8742–8746.

Thomsen, W.J., and W.A. Catterall. 1989. Localization of the receptor site for α-scorpion toxins by antibody mapping: implications for sodium channel topology. *Proc. Natl. Acad. Sci. USA.* 86:10161–10165.

Tikhonov, D.B., and B.S. Zhorov. 2007. Sodium channels: ionic model of slow inactivation and state-dependent drug binding. *Biophys. J.* 93:1557–1570.

Tomaselli, G.F., N. Chiamvimonvat, H.B. Nuss, J.R. Balser, M.T. Perez-Garcia, R.H. Xu, D.W. Orias, P.H. Backx, and E. Marban. 1995. A mutation in the pore of the sodium channel alters gating. *Biophys. J.* 68:1814–1827.

Townsend, C., and R. Horn. 1999. Interaction between the pore and a fast gate of the cardiac sodium channel. *J. Gen. Physiol.* 113:321–331.

Tsang, S.Y., R.G. Tsushima, G.F. Tomaselli, R.A. Li, and P.H. Backx. 2005. A multifunctional aromatic residue in the external pore vestibule of Na^+ channels contributes to the local anesthetic receptor. *Mol. Pharmacol.* 67:424–434.

Tsushima, R.G., R.A. Li, and P.H. Backx. 1997. Altered ionic selectivity of the sodium channel revealed by cysteine mutations within the pore. *J. Gen. Physiol.* 109:463–475.

Vedantham, V., and S.C. Cannon. 2000. Rapid and slow voltage-dependent conformational changes in segment IVS6 of voltage-gated Na^+ channels. *Biophys. J.* 78:2943–2958.

Wang, G.K., C. Quan, and S.Y. Wang. 1998. A common local anesthetic receptor for benzocaine and etidocaine in voltage-gated μ1 Na^+ channels. *Pflugers Arch.* 435:293–302.

Wang, S.Y., and G.K. Wang. 1999. Batrachotoxin-resistent Na^+ channels derived from point mutations in transmembrane segment D4-S6. *Biophys. J.* 76:3141–3149.

West, J.W., D.E. Patton, Y. Scheuer, Y. Wang, A.L. Goldin, and W.A. Catterall. 1992. A cluster of hydrophobic amino acid residues required for fast Na^+ channel inactivation. *Proc. Natl. Acad. Sci. USA.* 89:10910–10914.

Willow, M., T. Gonoi, and W.A. Catteral. 1985. Voltage clamp analysis of the inhibitory actions of diphenylhydantoin and carbamazepine on voltage-sensitive sodium channels in neuroblastoma cells. *Mol. Pharmacol.* 27:549–558.

Wimley, W.C., and S.H. White. 1996. Experimentally determined hydrophobicity scale for proteins at membrane interfaces. *Nat. Struct. Biol.* 3:842–848.

Xie, X.M., B. Lancaster, T. Peakman, and J. Garthwaite. 1995. Interaction of the antiepileptic drug lamotrigine with recombinant rat brain type IIA Na^+ channels and with native Na^+ channels in rat hippocampal neurons. *Pflugers Arch.* 430:437–446.

Yang, Y.-C., and C.-C. Kuo. 2002. Inhibition of Na^+ current by imipramine and related compounds: different binding kinetics as an inactivation stabilizer and as an open channel blocker. *Mol. Pharmacol.* 62:1228–1237.

Yang, Y.-C., and C.-C. Kuo. 2003. S4/D4 position determines status of the inactivation gate in Na^+ channels. *J. Neurosci.* 23:4922–4930.

Yang, Y.-C., and C.-C. Kuo. 2005. An inactivation stabilizer of the Na^+ channel acts as an opportunistic pore blocker modulated by external Na^+. *J. Gen. Physiol.* 125:465–481.

Yarov-Yarovoy, V., J. Brown, E.M. Sharp, J.J. Clare, T. Scheuer, and W.A. Catterall. 2001. Molecular determinants of voltage-dependent gating and binding of pore-blocking drugs in transmembrane segment IIIS6 of the Na^+ channel α subunit. *J. Biol. Chem.* 276:20–27.

Yarov-Yarovoy, V., J.C. McPhee, D. Idsvoog, C. Pate, T. Scheuer, and W.A. Catterall. 2002. Role of amino acid residues in transmembrane segments IS6 and IIS6 of the Na+ channel alpha subunit in voltage-dependent gating and drug block. *J. Biol. Chem.* 277:35393–35401.

Zamponi, G.W., and R.J. French. 1994. Transcainide causes two modes of open-channel block with different voltage sensitivities in batrachotoxin-activated sodium channels. *Biophys. J.* 67:1028–1039.

Zhang, J., T. Hadlock, A. Gent, and G.R. Strichartz. 2007. Tetracaine-membrane interactions: effects of lipid composition and phase on drug partitioning, location, and ionization. *Biophys. J.* 92:3988–4001.